Are economists getting climate dynamics right and does it matter?

Simon Dietz[1,2], Frederick van der Ploeg[2,3,4], Armon Rezai[2,5] and Frank Venmans[6,1]

February 6, 2020

Abstract

We show that several of the most important economic models of climate change produce climate dynamics inconsistent with the current crop of models in climate science. First, most economic models exhibit far too long a delay between an impulse of CO_2 emissions and warming. Second, few economic models incorporate positive feedbacks in the carbon cycle, whereby carbon sinks remove less CO_2 from the atmosphere, the more CO_2 they have already removed cumulatively, and the higher is temperature. These inconsistencies affect economic prescriptions to abate CO_2 emissions. Controlling for how the economy is represented, different climate models result in significantly different optimal CO_2 emissions. A long delay between emissions and warming leads to optimal carbon prices that are too low and too much sensitivity of optimal carbon prices to the discount rate. Omitting positive carbon cycle feedbacks also leads to optimal carbon prices that are too low. We conclude it is important for policy purposes to bring economic models in line with the state of the art in climate science.

Keywords: carbon cycle, carbon price, climate change, integrated assessment modelling, positive feedbacks, social cost of carbon

JEL codes: Q54

[1] London School of Economics and Political Science, London, UK

[2] CESifo, Munich, Germany

[3] University of Oxford, Oxford, UK

[4] Vrije Universiteit Amsterdam, Amsterdam, The Netherlands

[5] Vienna University of Economics and Business, Vienna, Austria; IIASA, Laxenburg, Austria

[6] University of Mons, Mons, Belgium

Email for correspondence: s.dietz@lse.ac.uk. We would like to acknowledge the financial support of the Grantham Foundation and FNRS. SD would also like to thank the Oxford Martin School at the University of Oxford, which hosted him for part of this research. The authors have no conflicts of interest or financial interests to disclose.

1 Introduction

Climate change is arguably the quintessential dynamic problem in economics. Carbon dioxide resides in the atmosphere for centuries after it is emitted, while the climate system operates on timescales ranging from seconds to millennia. Presumably climate dynamics must therefore be accurately represented in economic models of climate change, if appropriate policy prescriptions are to be made. But do economic models get climate dynamics right? To the extent that they don't, does it matter?

This paper aims to provide some answers to these two questions. First, we draw to the attention of the economics community some key inconsistencies between how leading economic models of climate change represent climate dynamics and how the current generation of climate science models does. Second, we explore the economic implications of these inconsistencies. Using the economic module of Nobel prize winner William Nordhaus' DICE model as a consistent representation of the economy, we quantify how different models of the climate system affect optimal CO_2 prices/taxes, CO_2 emissions and temperatures.

Section 2 elaborates on how the leading economic models of climate change fail to conform to climate science models and provides an explanation of the underlying dynamics we see in the climate science models. We select six economic models – the three most influential integrated assessment models or IAMs, together with three analytical models from prominent recent papers – and test how their climate modules respond in two experiments, compared with a large sample of 256 climate science models. The first test/experiment is of how fast and how far temperature rises in response to a CO_2 emission impulse. We show that the climate science models uniformly heat up very quickly to a constant, steady-state level, whereas the economic models heat up slowly and in some cases very slowly, and do not attain a steady-state temperature within two centuries. The second test is of how absorption of CO_2 by terrestrial and especially ocean carbon sinks changes as a function of how much CO_2 carbon sinks have already absorbed cumulatively, and of temperature. We show that Earth System models exhibit diminishing marginal uptake of CO_2 by carbon sinks with respect to atmospheric CO_2, which in turn is proportional to both cumulative CO_2 uptake by carbon sinks, and temperature. These constitute positive feedbacks in the carbon cycle. By contrast, most of the economic models exhibit *increasing* marginal uptake.

Section 3 offers a general framework to understand the models of the carbon cycle and warming process featured in these two experiments, both from climate science and economics. This framework enables us to decompose the dynamic temperature response to a CO_2 emission impulse in the models into the dynamic response of (i) the atmospheric CO_2 concentration and (ii) temperature. This decomposition demonstrates that the economic models vary widely in how fast a CO_2 emission impulse decays and how much is removed from the atmosphere in the long run. It also shows that the response of atmospheric CO_2 in the economic models generally differs from the representative climate science model. In particular, most models remove CO_2 from the atmosphere too slowly at first. The second part of the decomposition shows that almost all of the economic models exhibit too much temperature inertia in response to elevated atmospheric CO_2.

In Section 4, we move on to exploring the economic implications of different representations of the climate system, i.e. we turn to whether any of this matters for climate policy. We couple various models of the climate system with a common economic module, namely that of DICE. This is sufficient to illustrate in controlled conditions that different climate models result in significantly different optimal CO_2 emissions, concentrations and temperatures, both on emissions paths that maximise social welfare and on emissions paths that minimise CO_2 abatement costs subject to a 2°C warming constraint (per the UN Paris Agreement on Climate Change).

Since the various climate models differ in multiple ways, Section 5 isolates the effects of (i) too long a delay between emissions and warming and (ii) failing to simulate positive carbon cycle feedbacks. On the first, we find a long delay between an emission impulse and warming leads to optimal carbon prices that are too low. It also implies optimal carbon prices are too sensitive to the discount rate, since the costs of global warming are erroneously placed too far in the future. On the second, failing to simulate positive carbon cycle feedbacks also leads to optimal carbon prices that are too low. The effect is larger when cumulative CO_2 uptake and temperature are high and overall it is of comparable size to a long delay. Lastly it is worth noting that we specifically find DICE heats up too much in the long run and this contributes to the false impression that it is infeasible to limit warming to 2°C as mandated by the UN Paris Agreement.

Section 6 concludes and offers a discussion, including recommendations on how economists should proceed with representing the climate system in their models, depending on the complexity and purpose of those models.

2 Two key tests of climate dynamics

Perhaps contrary to popular belief, the temperature response to a CO_2 emission impulse in climate science models is *fast.* Figure 1 shows this. Peaking around ten years after the emission impulse, temperature is then permanently elevated. The response of the models resembles a step function. To produce this figure, we recreated a well-known experiment in climate science (Ricke and Caldeira, 2014), which has also been recommended by the US National Academy of Sciences as a key test of the consistency of economic models of climate change with current understanding in climate science (National Academies of Sciences, Engineering, and Medicine, 2017). We used reduced-form representations of 16 carbon cycle models and 16 atmosphere-ocean general circulation models to generate a set of 256 climate science models, each of which maps CO_2 emissions on to global mean surface temperature.[1] In this particular experiment, each model is subjected to an instantaneous emission impulse of 100 gigatonnes of carbon. To put this in context, 100GtC ($\approx$ 367GtCO_2) is equivalent to about ten years of CO_2 emissions from burning fossil fuels, at current levels (Le Quéré et al., 2018). This emission impulse is released in the models when the background atmospheric CO_2 concentration is 389 parts per million, which was the level observed in 2010.[2] The resulting distribution of model responses is the shaded area. Appendix A contains further details of the experiment.

[1]This set corresponds with the so-called CMIP5 ensemble, after the 5th Coupled Model Intercomparison Project of the World Climate Research Programme.

[2]https://data.giss.nasa.gov/modelforce/ghgases/Fig1A.ext.txt

Figure 1: Dynamic temperature response of 256 climate science models (the CMIP5 ensemble) and six economic models to an instantaneous 100GtC emission impulse against an initial background atmospheric CO_2 concentration of 389ppm. The temperature response of the economic models is much slower than the climate science models. After 200 years, the temperature response of the economic models is often well outside the range of the climate science models.

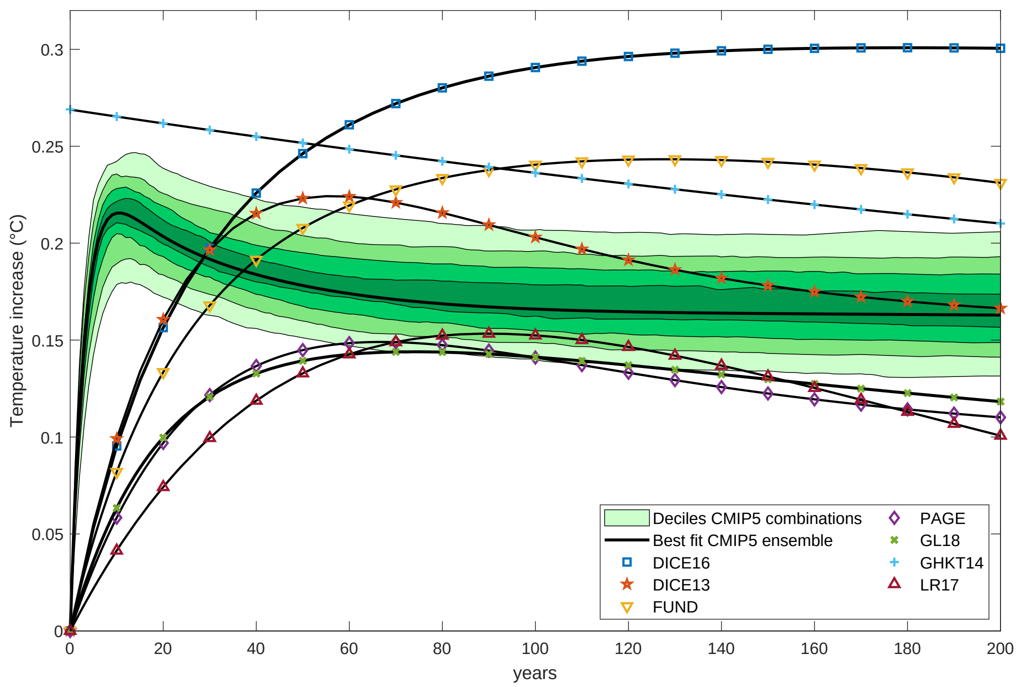

Why does the temperature response to a CO_2 emission impulse resemble a step function? It is due to two natural processes represented in climate science models almost exactly offsetting each other (see e.g. Matthews et al., 2009). One is the process of warming in response to an increase in atmospheric CO_2. The other is the process of a CO_2 emission impulse being removed from the atmosphere by ocean and terrestrial carbon sinks. Together these determine the temperature response to a ramp change in CO_2 emissions:

$$\frac{\Delta T_t}{\Delta E_0} = \int_0^t \frac{\Delta T_t}{\Delta M_s} \frac{\Delta M_s}{\Delta E_0} ds, \tag{1}$$

where $\Delta T_t/\Delta M_s$ is temperature change per unit increase of atmospheric CO_2 and $\Delta M_s/\Delta E_0$ is the increase in atmospheric CO_2 per unit of emissions. $\Delta T_t/\Delta M_s$ increases slowly, at a decreasing rate, because the oceans take up heat and slowly bring the system into equilibrium with an injection of energy. This is the widely known phenomenon of thermal inertia. Less well known, however, is that this thermal inertia is almost exactly offset by $\Delta M_s/\Delta E_0$ decreasing slowly, also at a decreasing rate, because of the slow absorption of atmospheric CO_2 by carbon sinks, principally the oceans. The reason why these processes almost exactly offset each other is thought to be that they are linked by the same mixing of surface and deep ocean waters (Matthews et al., 2009; Solomon et al., 2009; Goodwin et al., 2015; MacDougall and Friedlingstein, 2015). Dietz and Venmans (2019) provide further background.

Compared with the climate science models, Figure 1 shows that the climate modules contained in leading economic models of climate change do not exhibit the same behaviour. In particular, there is far too much delay between the injection of CO_2 and the resulting peak in warming in almost all the economic models. Thereafter, temperature begins to decrease again in many of the economic models, which is also contrary to the climate science models. For this part of the figure, we gathered the three most influential quantitative IAMs, namely DICE, FUND and PAGE.[3] As an example of their policy application, these models are used in the United States to estimate the social cost of carbon – the marginal damage cost of CO_2 – for the purposes of cost-benefit analysis of federal regulations (Interagency Working Group on Social Cost of Carbon, 2013). We include both the 2013 and 2016 iterations of the DICE model due to their divergent behaviour, as the figure clearly shows. We complement these three IAMs with three leading analytical climate-economy models published in recent years (Golosov et al., 2014; Gerlagh and Liski, 2018; Lemoine and Rudik, 2017). Of these, the model of Golosov et al. is particularly widely used. We implement the same experiment, injecting 100GtC into the models against a background atmospheric CO_2 concentration of 389ppm.[4] The temperature response peaks after 55 years in DICE 2013, 68 years in PAGE and 75 years in the model of Gerlagh and Liski (GL18). In the central case studied by Lemoine and Rudik (LR17) it takes 92 years, in FUND it takes 128 years and in DICE 2016 it takes 180 years. The only model that does not simulate a long delay is that of Golosov et al. (GHKT14),

[3] We include both DICE 2013 (Nordhaus, 2014) and DICE 2016 (Nordhaus, 2017), FUND3.11 (https://github.com/fund-model/MimiFUND.jl) and PAGE09 (Hope, 2013).

[4] All climate science and economic models have an equilibrium climate sensitivity of 3.1°C for this experiment. See Appendix A.

which assumes no delay in the temperature response *a priori*. This turns out to be a reasonable approximation.

In Figure 2, we move on to consider another key aspect of the climate response to CO_2 emissions: as the atmospheric CO_2 concentration increases, carbon sinks become less effective at removing CO_2 from the atmosphere. As the oceans warm up, they keep less CO_2 in solution and more stays in the atmosphere, thus further increasing temperature. CO_2 also reacts with seawater to form carbonic acid. This releases hydrogen ions, which combine with carbonate to form bicarbonate. This increases ocean acidity, destroys phytoplankton and the ability of the oceans to absorb carbon (Revelle and Suess, 1957). In addition, climate change is expected to reduce net uptake of CO_2 by plants and changes to the ocean circulation could also reduce CO_2 uptake (Friedlingstein et al., 2006). These processes constitute positive feedbacks in the carbon cycle (Collins et al., 2013).[5]

Most economic models of climate change do not take these feedbacks into account, however. Rather they assume that the rate of removal of a CO_2 emission impulse is independent of the background concentration of atmospheric CO_2. The exceptions are FUND and PAGE, both of which incorporate feedbacks from carbon sinks to atmospheric CO_2/warming. To evaluate the six economic models in this regard, we compare them with the FAIR (Finite Amplitude Impulse Response) model (Millar et al., 2017). Again, this comparison was identified by the National Academy of Sciences as a key test of the consistency of economic models of climate change with current understanding in climate science (National Academies of Sciences, Engineering, and Medicine, 2017). FAIR takes the same model structure contained in the 256 climate science models used above and introduces simple feedbacks from cumulative CO_2 uptake by carbon sinks and from temperature to reduced *marginal* uptake of atmospheric CO_2 by carbon sinks (see Section 3 for an exact description). FAIR was built to reproduce the behaviour of complex Earth System models and was widely used by IPCC in its recent *Special Report on Global Warming of 1.5°C* (Rogelj et al., 2018).

We calibrate the FAIR model to the mean climate science model depicted in Figure 1. We then run FAIR under a scenario of constant 2015 greenhouse gas emissions and plot yearly uptake of CO_2 by carbon sinks as a function of the atmospheric CO_2 concentration (Appendix A contains further details of this experiment). Without the carbon cycle feedbacks, yearly (i.e. marginal) removal

[5]Not included here are further positive greenhouse gas feedbacks such as permafrost thawing, which tend instead to be classed as tipping points in the climate system (Lenton et al., 2008).

of CO_2 would be proportional to atmospheric CO_2, simply due to Henry's law.[6] This explains why, in almost all of the economic models, there is an increasing relationship between atmospheric CO_2 and marginal CO_2 removal.[7] However, saturation of the ocean carbon sink, as well as other climate impacts on the effectiveness of carbon sinks, offsets this. In FAIR, this countervailing effect is large enough to produce a *decreasing* relationship between atmospheric CO_2 and marginal CO_2 removal overall. Atmospheric CO_2 is proportional to cumulative CO_2 uptake by carbon sinks and to temperature, which are the underlying drivers of the effect. The one economic model in which this is also the case is FUND, with its substantial carbon cycle feedback.

Figure 2: Yearly uptake of CO_2 by carbon sinks as a function of atmospheric CO_2 in FAIR and six economic models under constant 2015 greenhouse gas emissions. Each marker represents five years. FAIR shows yearly uptake decreases, while the economic models have it increasing, except FUND.

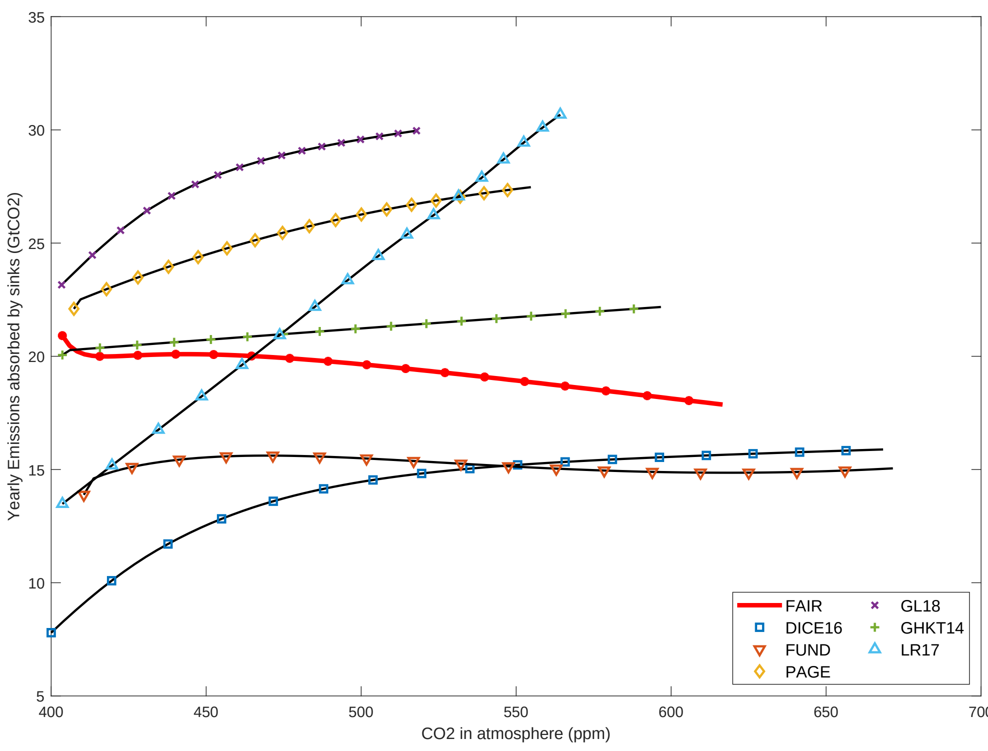

[6]The amount of dissolved gas in a liquid (i.e. the oceans) is proportional to its partial pressure above the liquid (i.e. in the atmosphere).

[7]This is easiest to see in the case of a one-box carbon cycle, such as that of Lemoine and Rudik (2017). $\dot{M} = E - \delta M$, where E stands for the flow of emissions and δ is the decay/removal rate. Yearly uptake δM is linearly proportional to M. In models with multiple boxes like DICE 2016, yearly uptake tends to increase at a decreasing rate due to the growing effect over time of the slow-decaying boxes. See Section 3 for further details.

There is reason to believe these two discrepancies between the current crop of climate science models and the leading economic models of climate change could matter for policy prescriptions. First, given the centrality of discounting in climate change economics (Arrow et al., 2013; Gollier, 2012; Nordhaus, 2007; Stern, 2007), the fact that economic models underestimate warming in the near future in response to a CO_2 emission impulse could significantly impact the welfare evaluation of emissions abatement responses. According to the climate science models, CO_2 emissions elevate temperatures almost immediately. Avoiding those emissions would therefore pay an almost immediate dividend. Second, ignoring the diminishing marginal effectiveness of carbon sinks underestimates the climate response to CO_2 emissions in the long run, which again impacts the welfare evaluation of emissions abatement responses.

3 Models of the carbon cycle and temperature dynamics

How do the models used in the previous section – both the climate science models and the economic models – actually work? In this section, we offer a general framework for understanding this. The framework enables us to decompose the dynamic temperature response to a CO_2 emission impulse in the models into the dynamic response of (i) the atmospheric CO_2 concentration and (ii) temperature, just as in the formula for the TCRE (1). By describing the models in more detail, we also set the scene for our subsequent economic analysis, which is based on coupling different climate models with the DICE economic module.

Linear models of the carbon cycle

Most simple models of the carbon cycle partition the system into a series of reservoirs or boxes, between which carbon is exchanged. The diffusion of carbon between n different boxes (e.g. the atmosphere, biosphere, upper and lower parts of the oceans) can be modelled by a system of n difference equations of the form

$$\mathbf{m}_t = \mathbf{A}\mathbf{m}_{t-1} + \mathbf{b}E_t, \tag{2}$$

where the vector $\mathbf{m}_t$ contains the stocks of carbon in each of the n boxes at the end of period t and the scalar E_t denotes CO_2 emissions during period t. $\mathbf{A}$ is a matrix whose elements describe the speed of diffusion between the boxes. The vector $\mathbf{b}$ contains the shares of emissions that enter each of the boxes. As the matrix $\mathbf{A}$ and the vector $\mathbf{b}$ are constant, (2) corresponds to a linear carbon cycle.

Define the aggregate stock of atmospheric carbon as $M_t \equiv \mathbf{d}'\mathbf{m}_t$. Then

$$M_t = \mathbf{d}' \left(\mathbf{A}^t M_0 + \sum_{s=1}^{t} \mathbf{A}^{t-s} \mathbf{b} E_s \right), \tag{3}$$

where M_0 is the initial stock of atmospheric carbon. We use spectral decomposition (see Appendix B) to obtain the response function

$$\Delta M_t = \sum_{s=1}^{t} \sum_{i=1}^{n} \psi_i \lambda_i^{t-s} \Delta E_s, \tag{4}$$

where the $\lambda_i \in \{0, 1\}$ are the eigenvalues of $\mathbf{A}$ in decreasing order of magnitude and the constants $\psi_i > 0$ are defined in Appendix B. If a proportion of emissions stays in the atmosphere forever, $\lambda_1 = 1$ for the box pertaining to that proportion ($i = 1$) and the impulse response is the sum of the permanent and transitory components,

$$\frac{\Delta M_t}{\Delta E_1} = \psi_1 + \sum_{i=2}^{n} \psi_i \lambda_i^{t-1}. \tag{5}$$

Thus the impulse response function (5) fully determines any linear carbon cycle model with any number of boxes, which explains why such impulse response functions are commonly used in climate science to represent and compare models of varying degrees of complexity. Table 1 summarises the carbon cycle models, which were compared in the previous section, using this general framework. Joos et al. (2013) is the representative climate science model, i.e. the model used to fit the CMIP5 ensemble (see Appendix A). While the number of boxes varies, most models are based on a structure in which there is a permanent box, into which roughly one fifth to one sixth of a CO_2 emission impulse flows, a very slowly decaying box and one or more boxes that decay much more quickly. However, there is significant variation in both the shares of emissions flowing into each box and the residence time (specifically the half-life) of CO_2 in each of the temporary boxes.[8]

What CO_2 dynamics do these different representations give rise to? Figure 3 plots the CO_2

[8] The shares flowing into the three boxes of the GL18 model do not add up to one, since only 94% of box 1 pertains to the atmosphere (the rest is assumed to be absorbed immediately by the upper ocean). The half-life of CO_2 in box 2 of DICE 2016 is much larger than in earlier versions of DICE, or in the other models shown.

Table 1: Comparing key linear carbon cycle models

Model	Time step (years)	Box				
		1. Permanent	2. Temporary	3. Temporary	4. Temporary	5. Temporary
DICE 2016	5	22%	41%; 851 years	37%; 9 years		
FUND	1	13%	20%; 252 years	32%; 51 years	25%; 12 years	10%; 1.4 years
PAGE	varies	19%	43%; 73 years	38%; < 1 years		
GHKT14	10	20%	31%; 300 years	49%; < 10 years		
GL18	10	16%	18%; 91 years	44%; 11 years		
LR17	1		100%; 50 years			
Joos et al. (2013) / best fit CMIP5 ensemble	1	22%	22%; 277 years	28%; 25 years	28%; 3 years	

Key: the first figure in each cell is the fraction of emissions flowing into box i (ψ_i) and the second figure the time it takes for half of the carbon to have left box i ($\ln(0.5)/\lambda_i$ for Joos et al. (2013) and timestep $\times \ln(0.5)/\ln(\lambda_i)$ for the other models). Both FUND and PAGE include additional positive carbon cycle feedbacks that are not included in this table.

Figure 3: Removal of a 100GtC emission impulse (47ppm CO_2) on an initial background concentration of 389ppm in climate science models and six economic models. There are big differences between the economic models. Few of the economic models approximate the best fit of the climate science model distribution.

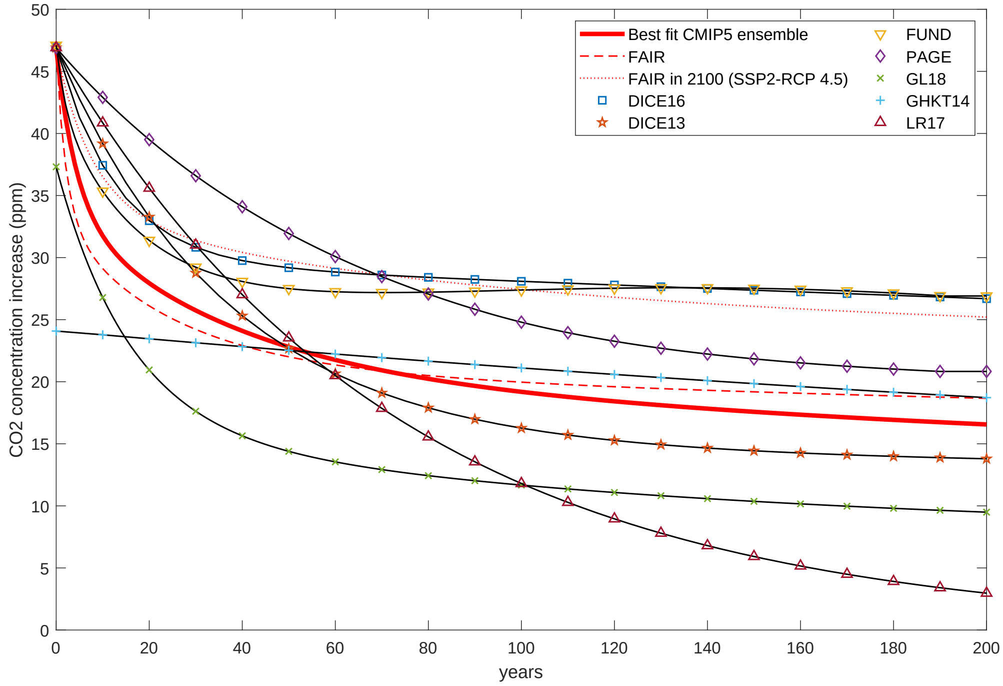

impulse responses of the various models. The impulse size is 100GtC as in the experiments above. The figure shows that the differences between the models' structures and parameters cause significant differences in their CO_2 impulse responses. Some models such as GL18 remove CO_2 very quickly initially. Others such as PAGE remove it very slowly. Over the first 50 years, however, most economic models remove CO_2 more slowly than the best fit of the CMIP5 ensemble. After a couple of centuries, some economic models such as LR17 remove most of the CO_2 emission impulse. Others such as DICE 2016 and FUND remove relatively little. By then, there does not appear to be a systematic bias between the economic models and the best fit of CMIP5. Overall, few of the economic models resemble the best fit of CMIP5, however.

As mentioned in Section 2, the biosphere and especially the ocean carbon sinks become decreasingly effective at removing CO_2 from the atmosphere, the more CO_2 has been taken up cumulatively and the higher is temperature. These positive feedbacks are not captured by the linear carbon cycles included in Table 1, which is clear from the fact that, although the CO_2 impulse response in Equation (5) decays with time, it does not depend on the atmospheric carbon stock. FAIR (Millar et al., 2017) was designed precisely to simulate these positive carbon cycle feedbacks by extending the four-box carbon cycle of Joos et al. (2013). The feedbacks in FAIR are based on the linear relationship that has been observed between the integrated CO_2 impulse response over 100 years, i.e. integrating the area under the curve in Figure 3 from $t = 0$ to 100, and both temperature and cumulative CO_2 emissions absorbed by carbon sinks:

$$\text{iIRF}_{100} = r_{pi} + r_T T + r_C \left[\sum_{s=pi}^{t} E_s - (M_s - M_{pi}) \right] \tag{6}$$

where $r_{pi} = 34.4$ years is the estimated pre-industrial value of iIRF_{100}. Here $\sum_{s=pi}^{t} E_s$ denotes cumulative CO_2 emissions since pre-industrial. The parameters $r_T = 4.165$ years/°C and $r_C = 0.019$ years/GtC capture the positive feedbacks from rising temperatures and cumulative carbon uptake respectively. Matching the integrated impulse response function from the carbon cycle model, modified for the positive feedback with iIRF_{100}, then determines a scaling factor α in FAIR that slows down the speed at which carbon is removed from the atmosphere (i.e. replace the λ_i with λ_i/α). Appendix A contains further details. Figure 3 shows FAIR's positive carbon cycle feedbacks in action: less CO_2 is removed from the atmosphere when the emission impulse is against a higher (year 2100) background concentration of CO_2.[9]

Temperature dynamics

From the carbon cycle models, the change in atmospheric CO_2 relative to pre-industrial determines radiative forcing, i.e. the change in the balance between incoming solar radiation and outgoing infra-red radiation in the Earth's atmosphere:

$$F_t = F_{\text{j}\times\text{CO}_2} \left(\log_j \frac{M_t}{M_{1750}} \right) + F_{\text{nonCO}_2,t}, \tag{7}$$

[9]Corresponding with the year 2100 on the IPCC's RCP4.5 scenario. RCP stands for Representative Concentration Pathway. IPCC developed four RCP scenarios for the *Fifth Assessment Report* (Moss et al., 2010).

Table 2: Comparing linear temperature-forcing responses

	Time step (years)	Box 1	Box 2
DICE 2016	5	9.9%; 25 years	0.2%; 150 years
FUND	1	100%; 31 years	
PAGE	varies	100%; 24 years	
GHKT14	10	n.a.	n.a.
GL18	10	100%; 34 years	
LR17	1	100%; 50 years	
Geoffroy et al. (2013) / best fit CMIP5 ensemble	1	13.5%; 3 years	0.2%; 167 years

Key: The first figure in each cell is the weight of each mode and the second figure the half-life for each mode. PAGE models regional temperature and calculates global temperature as the area-weighted average.

where F_t is radiative forcing, $F_{j\times CO_2}$ is a parameter representing the radiative forcing resulting from j times atmospheric CO_2 and $F_{\mathrm{nonCO_2},t}$ is radiative forcing from greenhouse gases other than CO_2, and from other forcing agents such as aerosols. In some models such as DICE, $F_{\mathrm{nonCO_2},t}$ is exogenous. In FUND and PAGE, $F_{\mathrm{nonCO_2},t}$ is determined endogenously by modelling the dynamics of some of the other greenhouse gases, such as methane and nitrous oxide. Either way, the contribution to total radiative forcing of gases/drivers other than CO_2 is non-trivial, of the order of 25% currently (IPCC, 2013). The concave, logarithmic relationship between radiative forcing and atmospheric CO_2 captures the fact that the absorption of radiation in CO_2's band becomes progressively saturated.

The temperature response to forcing is modelled by up to two temporary boxes and can be written analogously to (4) as

$$\Delta T_t = \sum_{s=1}^{t} \sum_{i=1}^{2} \psi_i^T \lambda_i^{T\, t-s} \Delta F_s, \tag{8}$$

where ψ_i^T and λ_i^T denote respectively the shares and eigenvalues for the temperature dynamics. Table 2 summarises the dynamics of the various warming models that map forcing into temperature. GHKT14 effectively assume that temperature is driven by equilibrium climate sensitivity according to Arrhenius' law and do not have any lag between forcing and temperature. GL18 have one box with a half-life of 34 years. Geoffroy et al. (2013) is the representative climate science model used to fit the CMIP5 ensemble. Both DICE 2016 and Geoffroy et al. (2013) have two boxes representing the temperature of the atmosphere/upper oceans and the deep oceans respectively. However, critically DICE 2016 displays a much more sluggish response of temperature to radiative forcing than Geoffroy et al. (2013), especially as the fast box of Geoffroy et al. has a half-life of only 3 years.

Figure 4 uses Equations (7) and (8) to plot the dynamic temperature response of the models to a *constant* increase in atmospheric CO_2 of 100GtC (47ppm). With the exception of Golosov et al. (2014), all of the economic models exhibit a more sluggish temperature response than the best fit of the CMIP5 ensemble. The temperature response of LR17 is particularly slow. After 200 years, temperature is higher in DICE 2013, DICE 2016 and FUND, while LR17 and PAGE are close to the best fit of the CMIP5 ensemble at that moment. The GHKT14 model shows an immediate, permanent increase in temperature. It over-predicts temperature compared with the best fit of the CMIP5 ensemble.

Figure 4: Dynamic temperature response of best-fit climate model and six economic models to a constant increase in atmospheric CO_2 of 100 GtC (47ppm CO_2). The economic models respond much more slowly to elevated CO_2 than the best-fit climate model, except GHKT14.

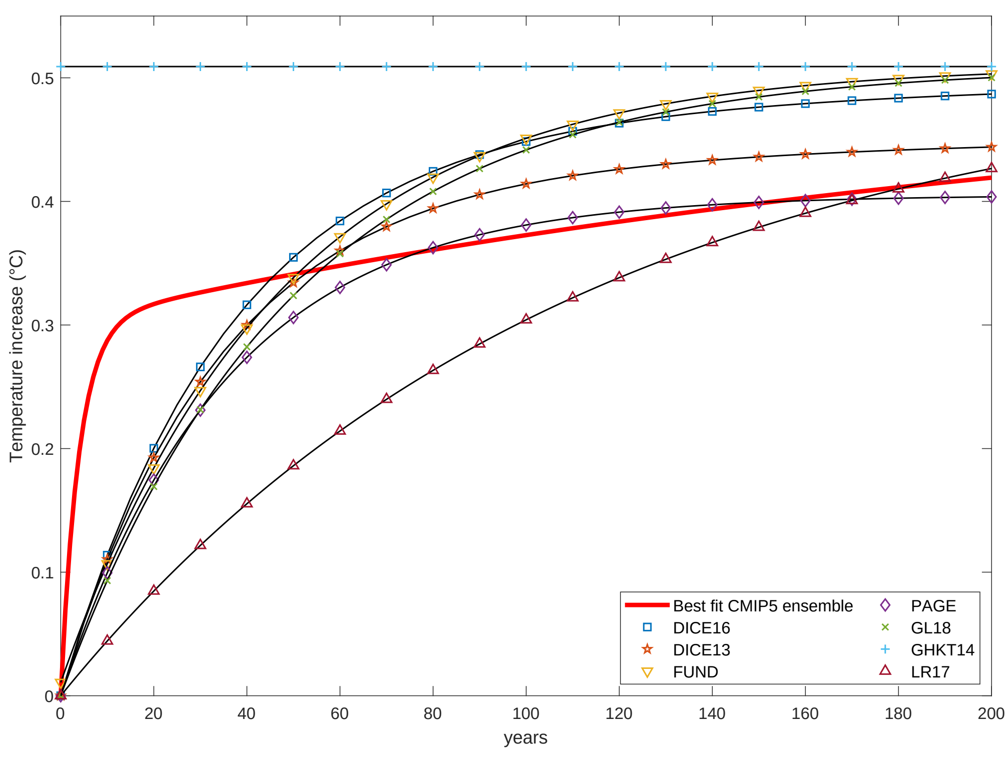

We emphasise the difference between this figure and Figure 1, which plots the dynamic temperature response of the models to a 100GtC emission impulse. Using Equations (5), (7) and (8),

Figure 1 plots

$$\frac{\Delta T_t}{\Delta E_1} = \frac{F_{2\text{xCO}_2}}{\ln 2} \sum_{s=1}^{t} \sum_{i=1}^{2} \psi_i^T \lambda_i^{T\ t-s} \frac{1}{M_s} \left(\psi_1 + \sum_{j=2}^{n} \psi_j \lambda_j^s \right), \tag{9}$$

i.e. carbon uptake as plotted in Figure 3 is convoluted with temperature inertia as plotted in Figure 4. The way in which temperature inertia almost exactly offsets dynamical carbon uptake in the best fit of the CMIP5 ensemble is visually clear from comparing Figures 3 and 4. That is why the temperature response in Figure 1 resembles a step function.

4 Economic policies with different climate models

In this and the following section, we evaluate what difference the model of the climate system makes for economic policies. We focus on two such policies: (i) optimal emissions that maximise social welfare and (ii) a representative policy run in the context of the United Nations climate framework that limits warming to 2°C at minimum discounted abatement cost. The latter path is sometimes described as an exercise in cost-effectiveness analysis (as opposed to (i), which is an exercise in cost-*benefit* analysis) and is a core use of IAMs by IPCC (see Clarke et al., 2014).[10]

To perform this evaluation, we need to make a controlled comparison, in which the models are identical in all respects except how they represent the dynamics of the carbon cycle and warming process. Control is achieved by using the DICE 2016 economic and welfare modules as a common base, and coupling it with different models of the climate system (Table 3).[11] We drop the FUND and PAGE models here, due to the practical difficulties of coupling these more complex IAMs with the DICE 2016 economy.

Figure 5 plots welfare-maximising carbon prices, emissions and temperatures (left column) from DICE 2016, DICE-FAIR-Geoffroy (i.e. the representative or benchmark climate science model, coupled with the DICE economy), DICE-GHKT14, DICE-GL18 and DICE-LR17. It is immediately apparent that the models differ significantly in their welfare-maximising paths. Initial carbon prices range from \$11/tCO_2 in DICE-LR17 to \$57 in DICE-GHKT14, with an initial carbon price of \$30 in the benchmark DICE-FAIR-Geoffroy model, and \$37 in standard DICE 2016. These differences

[10]Abatement cost minimisation subject to a temperature constraint is the same as welfare maximisation subject to a temperature constraint and ignoring climate damages.

[11]Readers are referred to William Nordhaus' web resources for a comprehensive description of the DICE 2016 economic module and, unless otherwise specified, the version we use is unchanged. See https://sites.google.com/site/williamdnordhaus/dice-rice.

Table 3: List and description of models used for economic evaluation

Model	Description
DICE 2016	Standard DICE 2016 economy and climate
DICE-GHKT14	DICE 2016 economy with the Golosov et al. (2014) climate model
DICE-GL18	DICE 2016 economy with the Gerlagh and Liski (2018) climate model
DICE-LR17	DICE 2016 economy with the Lemoine and Rudik (2017) climate model
DICE-FAIR-Geoffroy	DICE 2016 economy with the FAIR carbon cycle and the Geoffroy et al. (2013) warming model
DICE-Joos-Geoffroy	DICE 2016 economy with the Joos et al. (2013) carbon cycle and the Geoffroy et al. (2013) warming model

grow over time, such that by 2100 the range is \$77-358/tCO_2.

Welfare-maximising CO_2 emissions and temperatures also vary widely. Initial CO_2 emissions range from 33GtCO_2 in DICE-GHKT14 to 40GtCO_2 in DICE-LR17, while in 2100 they range from nearly zero to 50GtCO_2. Optimal warming by the end of the century ranges from just 2.0°C in DICE-LR17 to 4.0°C in DICE-GHKT14. Optimal warming in the benchmark DICE-FAIR-Geoffroy model is 3.0°C in 2100. Notice that optimal warming in 2100 is lowest in DICE-LR17, despite this model having the lowest carbon prices and the highest emissions. This is directly attributable to its particularly slow temperature response to elevated atmospheric CO_2, as shown in Figure 4. Notice also the high initial starting temperature in DICE-GHKT14. Temperature is only implicit in GHKT14, but can be backed out from their assumptions about the atmospheric carbon stock and damages. Their assumption of no delay between emissions and warming, coupled with exogenous radiative forcing from non-CO_2 greenhouse gases, leads to this artefactual result.

Figure 5 also compares models on a path that limits warming to 2°C at minimum discounted abatement cost (right column). Note that for these runs we substitute standard DICE 2016 exogenous emissions of CO_2 from land-use change and forestry with corresponding emissions from the IPCC's RCP2.6 scenario[12], which is consistent with limiting warming to 2°C. We do the same for exogenous radiative forcing from other greenhouse gases and atmospheric agents. We provide some further analysis of this issue below.

Similar to the models' welfare-maximising paths, we observe large differences in their 2°C cost-minimising paths. Naturally, given the warming constraint, the differences are particularly evident in carbon prices and emissions. Initial carbon prices vary from \$13/tCO_2 in DICE-LR17 to \$143

[12]Specifically when combined with the SSP1 socio-economic scenario; see Moss et al. (2010).

Figure 5: Welfare-maximising (left) and cost-minimising (right) paths from different climate models coupled with the DICE 2016 economy. Top row – carbon prices; middle row – CO_2 emissions; bottom row – warming. The models produce very different carbon price paths, resulting in very different CO_2 emissions and temperature paths.

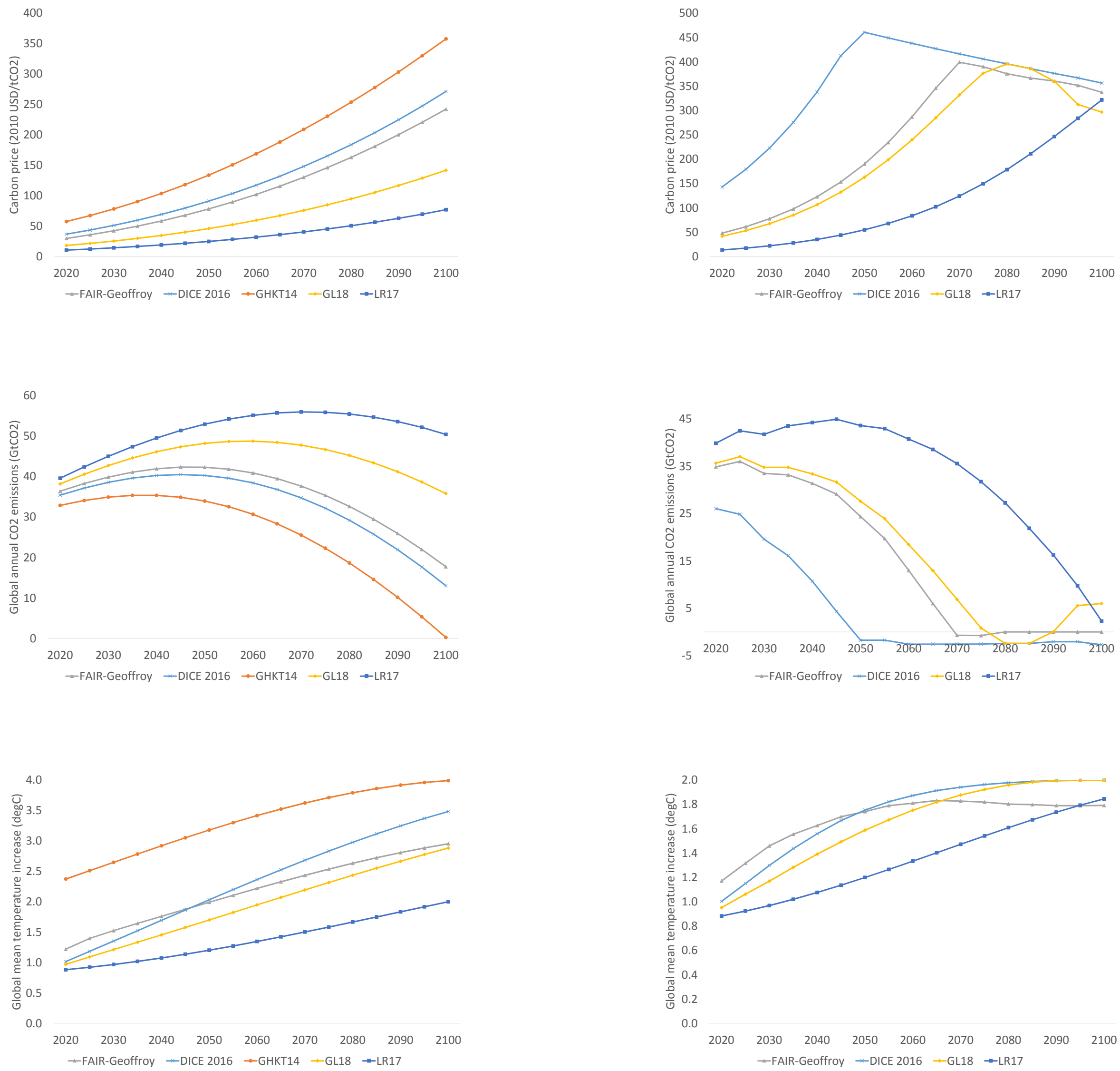

in standard DICE 2016. By mid-century the range of carbon prices peaks at \$406/tCO_2 between these models. Initial CO_2 emissions range from 26GtCO_2 in DICE 2016 to 40GtCO_2 in DICE-LR17. Limiting warming to 2°C is infeasible in DICE-GHKT14, for the reasons mentioned above. In order to limit warming to 2°C, emissions must eventually be negative in all models, but the time at which 'net zero' is crossed ranges from 2050 in DICE 2016 to just after 2100 in DICE-LR17. Although warming is limited to 2°C, the temperature trajectory shows significant variation across the models, particularly in mid-century. The range is 1.2-1.8°C in 2050, for instance.

5 Warming delay and further economic analysis

While Figure 5 illustrates that climate dynamics matter for economic policies, it does not fully illuminate the role of the issues identified in Section 2, namely the excessive delay between a CO_2 emission impulse and warming, and the omission of diminishing marginal CO_2 uptake with respect to warming. These issues are explored further in Tables 4 and 5.

To isolate the effect of excessive delay between a CO_2 emission impulse and warming, we construct two further artefact models, built on the DICE-Joos-Geoffroy (and DICE 2016) structure. These two models exhibit the same long-run temperature response to a CO_2 emission impulse as DICE-Joos-Geoffroy, but reach that long-run response at very different speeds; far too slowly in comparison with the climate science models, more in line with the economic models. The reason we construct these two further models is that, even with the same equilibrium climate sensitivity, the different climate models compared above exhibit not only different short- and medium-run temperature dynamics, they also exhibit different long-run temperature responses (as is clear from Figure 1), due to differences in long-run CO_2 uptake (as shown in Figure 3). The new 'Delay 56' model is so called, because it exhibits a delay between the CO_2 emission impulse and peak warming of 56 years, rather than c. 10 years in DICE-Joos-Geoffroy, while exhibiting a similar integrated temperature impulse response over the long run. The 'Delay 112' model exhibits a corresponding warming delay of 112 years. As explained in Appendix B, these new models are created by increasing the effective heat capacity of the ocean in the Geoffroy et al. (2013) model, whilst decreasing the rate of removal of CO_2 from the three temporary boxes in the Joos et al. (2013) carbon cycle.

Using these new models, Table 4 shows that on the welfare-maximising path an excessive delay leads to lower carbon prices throughout. The 2020 carbon price falls from \$27/tCO_2 for the short delay (DICE-Joos-Geoffroy) to \$23 for the 56-year delay and \$18 for the 112-year delay (compare rows 2-4). These differences grow over the course of the century. By 2100, moving from a 10-year delay to a 112-year delay reduces the optimal carbon price by \$75, or 38%. With lower carbon prices naturally come higher CO_2 emissions, but not higher temperatures, since a longer delay means that it takes much longer for the warming effect of these additional emissions to be realised. Table 5 shows that on the 2°C cost-minimising path an excessive delay leads to lower carbon prices in 2020 and 2050. The effect is somewhat smaller than on the optimal path, since the temperature constraint binds and leaves less room for manoeuvre. Lower carbon prices again result in higher emissions, but the delay means this does not translate into higher temperatures; on the contrary.

An implication of these results on excessive delay is that the optimal path may be less sensitive to assumptions about the discount rate than previously thought. Table 6 shows that this is indeed the case. We ran DICE-Joos-Geoffroy and the Delay 56 and 112 variants under standard DICE assumptions about the primitives of the social rate of time preference (a pure rate of time preference of 1.5% and an elasticity of marginal utility of consumption of 1.45), and assuming the social planner uses lower values (PRTP=0.1%; elasticity of marginal utility of 1). We call the latter 'public' discounting.[13] The parameter values are the same as in the *Stern Review* (Stern, 2007). With a representative initial growth rate of global average consumption per capita of 2.5%, the standard DICE discount rate is 5.1% while the 'public' discount rate is 3.5%. Table 6 shows that the increase in the 2020 optimal carbon price brought about by switching from standard to public discounting is 68% in Delay 112, but only 50% in DICE-Joos-Geoffroy with the short delay. In 2100 the increases are 51% and 38% respectively.

We now analyse how positive feedbacks in the carbon cycle affect model paths, by comparing DICE-FAIR-Geoffroy and DICE-Joos-Geoffroy (rows 1 and 2). Recall the difference between these models is that DICE-FAIR-Geoffroy modifies the four-box carbon cycle of Joos et al. (2013) to incorporate feedbacks from both cumulative carbon uptake and temperature to the rate of removal of atmospheric CO_2 (see Section 3). So DICE-FAIR-Geoffroy includes the feedbacks, while DICE-Joos-Geoffroy does not.

Introducing the positive feedbacks to the carbon cycle results in a higher optimal carbon price. In 2020, the optimal carbon price in DICE-FAIR-Geoffroy is \$29.68/tCO_2, \$2.70 above the optimal carbon price in DICE-Joos-Geoffroy. Hence the effect is not quantitatively large in the short run. However, it is in the nature of the carbon cycle feedbacks that they have a larger effect, the higher is the atmospheric carbon stock/temperature, so we see the gap between the models' optimal carbon

[13] We assume private agents keep the standard DICE parameters for investment/consumption decisions, but that the social planner sets carbon prices using the lower rate (van der Ploeg and Rezai, 2019).

Table 4: Welfare-maximising paths with variants of the DICE model. Comparing DICE-Joos-Geoffroy to Delay 56 and Delay 112 shows that an excessive warming delay results in lower carbon prices, higher CO_2 emissions, but lower temperatures. Comparing DICE-FAIR-Geoffroy (with positive carbon cycle feedbacks) to DICE-Joos-Geoffroy (no feedbacks) shows that positive feedbacks result in higher carbon prices, particularly in the long run, lower emissions and temperatures.

				2020	2050	2100	2020	2050	2100	2020	2050	2100
	Model	Carbon-cycle feedback	Temp. model	Carbon price (USD/tCO_2)			CO_2 emissions ($GtCO_2$)			Warming (°C)		
1	DICE-FAIR-Geoffroy	Yes	Short delay	29.68	78.17	242.18	36.37	42.28	17.75	1.22	1.99	2.95
2	DICE-Joos-Geoffroy	No	Short delay	26.97	66.53	197.61	36.76	44.23	25.28	1.25	2.08	3.01
3	Delay 56	No	Long delay	23.02	55.45	159.01	37.35	46.28	32.38	0.98	1.81	2.93
4	Delay 112	No	Long delay	17.88	42.17	122.98	38.19	48.91	39.68	0.92	1.52	2.67
5	DICE 2016	No	Long delay + too hot later	36.72	91.04	271.34	35.40	40.25	13.07	1.02	2.03	3.48

Table 5: 2°C cost-minimising paths in variants of the DICE model. Comparing DICE-Joos-Geoffroy to Delay 56 and Delay 112 shows that an excessive warming delay results in lower carbon prices and higher emissions in 2020 and 2050, but lower temperatures. Comparing DICE-FAIR-Geoffroy (with positive carbon cycle feedbacks) to DICE-Joos-Geoffroy (no feedbacks) shows that positive feedbacks result in higher carbon prices in 2020 and 2050, lower emissions and temperatures.

				2020	2050	2100	2020	2050	2100	2020	2050	2100
	Model	Carbon-cycle feedback	Temp. model	Carbon price (USD/tCO_2)			CO_2 emissions (GtCO_2)			Warming (°C)		
1	DICE-FAIR-Geoffroy	Yes	Short delay	47.98	189.91	337.33	34.88	24.38	0.00	1.17	1.74	1.79
2	DICE-Joos-Geoffroy	No	Short delay	41.62	167.56	337.34	35.65	27.05	0.00	1.20	1.84	1.89
3	Delay 56	No	Long delay	39.41	159.58	318.24	35.93	28.03	2.79	0.97	1.66	2.00
4	Delay 112	No	Long delay	35.83	140.72	357.64	36.40	30.44	-2.79	0.91	1.43	1.96
5	DICE 2016	No	Long delay + too hot later	142.95	460.68	356.31	26.05	-1.76	-2.71	1.00	1.67	2.00

Table 6: Sensitivity of optimal carbon prices to the discount rate. The longer is the warming delay, the more sensitive optimal carbon prices are to a change in the discount rate.

Model	Discount	2020	2030	2040	2050	2060	2070	2080	2090	2100
DICE-Joos-Geoffroy	Standard	26.97	37.55	50.64	66.53	85.52	107.86	133.86	163.72	197.61
	Public	40.45	53.20	71.53	94.24	121.13	152.31	187.95	228.20	273.12
	% diff.	**50.0**	**41.7**	**41.3**	**41.6**	**41.6**	**41.2**	**40.4**	**39.4**	**38.2**
Delay 56	Standard	23.02	31.79	42.54	55.45	70.73	88.55	109.12	132.57	159.01
	Public	36.59	47.44	63.25	82.70	105.50	131.68	161.29	194.30	230.49
	% diff.	**59.0**	**49.2**	**48.7**	**49.1**	**49.2**	**48.7**	**47.8**	**46.6**	**44.9**
Delay 112	Standard	17.88	24.38	32.41	42.17	53.82	67.56	83.57	102.00	122.98
	Public	30.07	38.09	50.46	65.93	84.25	105.41	129.46	156.41	186.10
	% diff.	**68.2**	**56.3**	**55.7**	**56.4**	**56.5**	**56.0**	**54.9**	**53.3**	**51.3**

prices widening steadily until by 2100 it is \$83/tCO_2. Higher optimal carbon prices result in lower emissions in DICE-FAIR-Geoffroy and this in turn results in lower 21st-century warming.[14] Reduced CO_2 uptake by carbon sinks reduces the cumulative emissions budget for limiting warming to 2°C in DICE-FAIR-Geoffroy, so the 2°C cost-minimising carbon price is also higher, resulting in lower emissions and, at least in this century, lower temperatures.

Tables 4 and 5 show that DICE 2016 yields higher carbon prices than the benchmark climate science model, DICE-FAIR-Geoffroy (compare rows 1 and 5), particularly on a 2°C cost-minimising path. This leads to lower emissions in DICE 2016, yet temperatures end up being higher. Appendix C provides some further analysis of what is behind the difference between standard DICE 2016 and DICE-FAIR-Geoffroy. Three factors are at play, namely differences in: (a) temperature dynamics between standard DICE 2016 and Geoffroy et al. (2013); (b) removal of atmospheric CO_2 between the DICE 2016 and Joos et al. (2013) carbon cycles, and; (c) assumptions about (non-)diminishing uptake of atmospheric CO_2 between DICE 2016/Joos et al. (2013) and FAIR. In Appendix C, we apportion the difference between (a)-(c) and find that the main driver of different temperatures is (a) the tendency of DICE 2016 to heat up too much in the long run.

Lastly, previous work with DICE 2016 found it is infeasible to limit warming to 2°C (Nordhaus, 2017).[15] Our analysis suggests this is not the case when the climate system is appropriately responsive to CO_2 emissions. Figure 5 and Table 5 show that doing so is feasible in DICE 2016, but very expensive, while it is also feasible in DICE-FAIR-Geoffroy, and much less expensive. Another reason why limiting warming to 2°C has been infeasible in DICE 2016 is the assumption in previous studies of one-size-fits-all exogenous emissions of CO_2 from land-use change and forestry, and exogenous radiative forcing from other greenhouse gases and atmospheric agents.[16] When DICE 2016 is run under standard DICE 2016 exogenous emissions/forcing, limiting warming to 2°C is indeed infeasible. It remains feasible in DICE-FAIR-Geoffroy, but much more expensive than under our preferred scenario for exogenous emissions/forcing (see Appendix C).

[14] Warming is higher in DICE-FAIR-Geoffroy in the longer run, due to the carbon cycle feedbacks' continuing effect. The crossing point is 2200 (not shown). In steady state, optimal warming in DICE-FAIR-Geoffroy is exactly 3°C, while in DICE-Joos-Geoffroy it peaks at about 2.83°C.

[15] Under the constraint of no negative emissions technology in the first several decades.

[16] One-size-fits-all in the sense of the scenario being invariant to the amount of CO_2 being abated in the model.

6 Discussion

We have investigated how best to fit the dynamic evolution of atmospheric carbon and temperature in the big Earth System models in climate science. Closely following experimental protocols developed in climate science, we have used reduced-form impulse response functions to emulate the behaviour of an ensemble of highly non-linear and large-scale Earth System models. In this sense, we have been concerned with the most appropriate model reduction techniques.

We have not been concerned with fitting our reduced-form models to historical data. This would have been a different exercise and the resulting model would be of limited relevance for the analysis of climate policy today. A model calibrated on historical conditions and designed to reproduce the behaviour of the pre-industrial climate, or the climate between pre-industrial times and the more recent past, is not a reliable model of the future climate. One important reason why is that positive feedbacks in the uptake of atmospheric carbon, studied in some depth in this paper, kick in more strongly when cumulative carbon uptake and temperature are already high (e.g. Millar et al., 2017). This partly explains why climate scientists tend to use the dynamic behaviour of Earth System models in simulation experiments in contemporary and future climatic conditions as their benchmark when building reduced-form models, not past, observed changes in atmospheric carbon and temperature.[17]

We have shown that there is a large amount of variation in the way economic models of climate change simulate the evolution of the atmospheric carbon stock and temperature. But still the most prominent IAMs, i.e. DICE, FUND and PAGE, as well as the analytical models put forward by Gerlagh and Liski (2018) and Lemoine and Rudik (2017), are unified in one feature. They show too sluggish a temperature response to an impulse change in CO_2 emissions compared with the step-like response of the large Earth System models and the reduced-form representations of those Earth System models used by climate scientists (e.g. Geoffroy et al., 2013; Joos et al., 2013; Millar et al., 2017). Unique among the economic models, Golosov et al. (2014) have an instant temperature response to changes in the atmospheric carbon stock, since they do not allow for a temperature lag at all. We have decomposed this sluggish temperature response into two underlying discrepancies

[17] That being said, Millar et al. (2017) show that the FAIR model, with its flexible representation of positive carbon cycle feedbacks, closely tracks observed global mean temperature when run with estimated historical greenhouse gas emissions.

between the economic models and their climate science counterparts. First, most economic models remove CO_2 from the atmosphere too slowly initially. Second, most economic models exhibit too much temperature inertia. The dominant half-life for the temperature dynamics of climate science models is 3 years, whilst for DICE 2016, Gerlagh and Liski (2018) and Lemoine and Rudik (2017), for instance, these half-lives are 25, 34 and 50 years, respectively. Besides the sluggish temperature response to CO_2 emissions, economic models also imply that the marginal removal of atmospheric CO_2 rises with atmospheric CO_2 (except for FUND), whilst carbon cycle models in climate science suggest that this removal decreases with atmospheric CO_2 (Millar et al., 2017).

As a result, the models of the climate that prevail in the economic literature yield misleading policy implications. Controlling for the specification of the economy and welfare using the DICE 2016 economic module, we found that the climate modules in economic models delivered carbon prices, emissions and temperatures that differed significantly from the benchmark FAIR model from climate science. We explored both welfare-maximising carbon prices and carbon prices that ensure a 2°C temperature target is achieved whilst minimising the costs of abatement. Further exploring the causes of these differences, we found that a sluggish temperature response to CO_2 emissions – excessive delay – leads to carbon prices that are too low and that are too sensitive to the choice of discount rate, since the costs of global warming are erroneously placed too far in the future. We also found that failing to account for positive feedbacks in the carbon cycle leads to carbon prices that are too low, especially when atmospheric CO_2 is high.

We conclude economic models of climate change are out of line with the state of the art in climate science. We therefore recommend the climate modules in economic models be replaced. Models of the carbon cycle need to incorporate positive feedback effects, like FAIR does (Millar et al., 2017). Models of temperature dynamics need to either be replaced or recalibrated so that they can reproduce the fast temperature response of Earth System models to CO_2 emissions, as the model of Geoffroy et al. (2013) does. Appendix D provides GAMS code for doing so in DICE. Other simple models in climate science may do the same job. None of these changes requires significant complication of existing economic models.

In fact, if future CO_2 emissions are not too high, an even simpler model where temperature is just a linear function of cumulative CO_2 emissions has been shown to suffice (Collins et al., 2013). Appendix E demonstrates this: the climate science models of CMIP5 exhibit an approximately linear warming response to cumulative CO_2 emissions under various IPCC emissions scenarios. The linear response requires a step temperature impulse response function and positive carbon cycle feedbacks (Dietz and Venmans, 2019). Hence Appendix E shows that the economic models covered in this paper do not generate a linear response. The CMIP5 ensemble gives temperature at time t as 1°C plus 1.6°C per trillion tons of cumulative emissions (TtC) from 2020 onwards (Stocker et al., 2013).[18] Warming from non-CO_2 greenhouse gases needs to be added on top. The slope coefficient of 1.6°C/TtC is known as the Transient Climate Response to Cumulative Carbon Emissions (TCRE).[19] However, at warming of over 4°C, this simple relationship may no longer hold (MacDougall, 2016) and one may need to use a more complicated model, such as FAIR in tandem with the temperature dynamics model of Geoffroy et al. (2013).

[18]Some recent studies that have used this simple relationship to derive economically optimal climate policies are Allen (2016), Brock and Xepapadeas (2017), van der Ploeg (2018), Manoussi et al. (2018) and Dietz and Venmans (2019).

[19]The simple formula whereby warming = TCRE x cumulative emissions implies a temperature response function to a CO_2 emission impulse that is approximated by a step function with amplitude equal to the TCRE. The temperature response function that best fits the CMIP5 ensemble in the experiment reported in Figure 1 has a mean amplitude of 1.72°C/TtC, while FAIR has a mean amplitude of 1.77°C/TtC under 2015 conditions. The differences between these values and the value of 1.6°C/TtC reported above and due to IPCC is down to the equilibrium climate sensitivity, which we harmonise to the default value of 3.1°C in DICE when producing Figure 1. The models synthesised for IPCC by Stocker et al. (2013) exhibit slightly lower values. Equilibrium climate sensitivity is the largest source of uncertainty about the TCRE. Matthews et al. (2009) found a 5-95% probability range of 1.0-2.1°C/TtC, Allen et al. (2009) found 1.4-2.5°C/TtC and Gillett et al. (2013) found 0.7-2.0°C/TtC based on the CMIP5 ensemble. Based on this and other evidence, IPCC adopted a 'likely' range of 1.0-2.1°C/TtC (Collins et al., 2013).

References

Aengenheyster, Matthias, Qing Yi Feng, Frederick Van Der Ploeg, and Henk A Dijkstra, "The point of no return for climate action," *Earth System Dynamics*, 2018, *9* (3).

Allen, Myles R, "Drivers of peak warming in a consumption-maximizing world," *Nature Climate Change*, 2016, *6*, 684–686.

_ **, David J Frame, Chris Huntingford, Chris D Jones, Jason A Lowe, Malte Meinshausen, and Nicolai Meinshausen**, "Warming caused by cumulative carbon emissions towards the trillionth tonne," *Nature*, 2009, *458* (7242), 1163–1166.

Arrow, Kenneth, Maureen Cropper, Christian Gollier, Ben Groom, Geoffrey Heal, Richard Newell, William Nordhaus, Robert Pindyck, William Pizer, Paul Portney et al., "Determining benefits and costs for future generations," *Science*, 2013, *341* (6144), 349–350.

Brock, William and Anastasios Xepapadeas, "Climate change policy under polar amplification," *European Economic Review*, 2017, *99*, 93–112.

Clarke, L., K. Jiang, K. Akimoto et al., "Asessing transformation pathways," in O. Edenhofer, R. Pichs-Madruga, Y. Sokona et al., eds., *Climate Change 2014: Mitigation of Climate Change. Contribution of Working Group III to the Fifth Assessment Report of the Intergovernmental Panel on Climate Change*, Cambridge, UK and New York, NY, USA: Cambridge University Press, 2014.

Collins, M., R. Knutti, J. Arblaster, J.-L. Dufresne, T. Fichefet, P. Friedlingstein, X. Gao, W.J. Gutowski, T. Johns, G. Krinner, M. Shongwe, C. Tebaldi, Weaver A.J., and M. Wehner, "Long-term climate change: projections, commitments and irreversibility," in T.F. Stocker, C. Qin, G.-K. Plattner, M. Tignor, S.K. Allen, J. Boschung, A. Nauels, Y. Xia, V. Bex, and P.M. Midgeley, eds., *Climate Change 2013: The Physical Science Basis. Contribution of Working Group I to the Fifth Assessment Report of the Intergovernmental Panel on Climate Change*, Cambridge, UK and New York, NY, USA: Cambridge University Press, 2013.

Dietz, Simon and Frank Venmans, "Cumulative carbon emissions and economic policy: in search of general principles," *Journal of Environmental Economics and Management*, 2019, *96*, 108–129.

Friedlingstein, Pierre, Peter Cox, Richard Betts, Laurent Bopp, Werner von Bloh, Victor Brovkin, Patricia Cadule, Scott Doney, Michael Eby, Inez Fung et al., "Climate-carbon cycle feedback analysis: results from the C4MIP model intercomparison," *Journal of Climate*, 2006, *19* (14), 3337–3353.

Geoffroy, Olivier, David Saint-Martin, Dirk JL Olivié, Aurore Voldoire, Gilles Bellon, and Sophie Tytéca, "Transient climate response in a two-layer energy-balance model. Part I: Analytical solution and parameter calibration using CMIP5 AOGCM experiments," *Journal of Climate*, 2013, *26* (6), 1841–1857.

Gerlagh, Reyer and Matti Liski, "Consistent climate policies," *Journal of the European Economic Association*, 2018, *16* (1), 1–44.

Gillett, Nathan P, Vivek K Arora, Damon Matthews, and Myles R Allen, "Constraining the ratio of global warming to cumulative CO2 emissions using CMIP5 simulations," *Journal of Climate*, 2013, *26* (18), 6844–6858.

Gollier, Christian, *Pricing the Planet's Future: The Economics of Discounting in an Uncertain World*, Princeton University Press, 2012.

Golosov, Mikhail, John Hassler, Per Krusell, and Aleh Tsyvinski, "Optimal taxes on fossil fuel in general equilibrium," *Econometrica*, 2014, *82* (1), 41–88.

Goodwin, Philip, Richard G Williams, and Andy Ridgwell, "Sensitivity of climate to cumulative carbon emissions due to compensation of ocean heat and carbon uptake," *Nature Geoscience*, 2015, *8* (1), 29–34.

Hope, Chris, "The marginal impact of CO2 from PAGE2002: An integrated assessment model incorporating the IPCC's five reasons for concern," *Integrated Assessment*, 2006, *6* (1).

_ , "The social cost of CO2 from the PAGE09 model," *Economics Discussion Papers*, 2011, (2011-39).

— , "Critical issues for the calculation of the social cost of CO2: why the estimates from PAGE09 are higher than those from PAGE2002," *Climatic Change*, 2013, *117* (3), 531–543.

Interagency Working Group on Social Cost of Carbon, "Technical update on the social cost of carbon for regulatory impact analysis under executive order 12866," Technical Report, Interagency Working Group on Social Cost of Carbon, United States Government 2013.

IPCC, *Climate Change 2013: The Physical Science Basis. Contribution of Working Group I to the Fifth Assessment Report of the Intergovernmental Panel on Climate Change*, Cambridge, United Kingdom and New York, NY, USA: Cambridge University Press, 2013.

Joos, Fortunat, Raphael Roth, JS Fuglestvedt, GP Peters, IG Enting, W von Bloh, V Brovkin, EJ Burke, M Eby, NR Edwards et al., "Carbon dioxide and climate impulse response functions for the computation of greenhouse gas metrics: a multi-model analysis," *Atmospheric Chemistry and Physics*, 2013, *13* (5), 2793–2825.

Lemoine, Derek and Ivan Rudik, "Steering the climate system: using inertia to lower the cost of policy," *American Economic Review*, 2017, *107* (10), 2947–57.

Lenton, Timothy M, Hermann Held, Elmar Kriegler, Jim W Hall, Wolfgang Lucht, Stefan Rahmstorf, and Hans Joachim Schellnhuber, "Tipping elements in the Earth's climate system," *Proceedings of the National Academy of Sciences*, 2008, *105* (6), 1786–1793.

MacDougall, Andrew H, "The transient response to cumulative CO2 emissions: a review," *Current Climate Change Reports*, 2016, *2* (1), 39–47.

— **and Pierre Friedlingstein**, "The origin and limits of the near proportionality between climate warming and cumulative CO2 emissions," *Journal of Climate*, 2015, *28* (10), 4217–4230.

Maier-Reimer, Ernst and Klaus Hasselmann, "Transport and storage of CO_2 in the ocean: an inorganic ocean-circulation carbon cycle model," *Climate dynamics*, 1987, *2* (2), 63–90.

Manoussi, Vassiliki, Anastasios Xepapadeas, and Johannes Emmerling, "Climate engineering under deep uncertainty," *Journal of Economic Dynamics and Control*, 2018, *94*, 207–224.

Matthews, H Damon, Nathan P Gillett, Peter A Stott, and Kirsten Zickfeld, "The proportionality of global warming to cumulative carbon emissions," *Nature*, 2009, *459* (7248), 829–832.

Millar, Richard J, Zebedee R Nicholls, Pierre Friedlingstein, and Myles R Allen, "A modified impulse-response representation of the global near-surface air temperature and atmospheric concentration response to carbon dioxide emissions," *Atmospheric Chemistry and Physics*, 2017, *17* (11), 7213–7228.

Moss, Richard H, Jae A Edmonds, Kathy A Hibbard, Martin R Manning, Steven K Rose, Detlef P Van Vuuren, Timothy R Carter, Seita Emori, Mikiko Kainuma, Tom Kram et al., "The next generation of scenarios for climate change research and assessment," *Nature*, 2010, *463* (7282), 747–756.

National Academies of Sciences, Engineering, and Medicine, *Valuing Climate Damages: Updating Estimation of the Social Cost of Carbon Dioxide*, National Academies Press, 2017.

Nordhaus, William D, "A review of the "Stern Review on the Economics of Climate Change"," *Journal of Economic Literature*, 2007, *45*, 686–702.

_ , "Estimates of the social cost of carbon: concepts and results from the DICE-2013R model and alternative approaches," *Journal of the Association of Environmental and Resource Economists*, 2014, *1* (1/2), 273–312.

_ , "Revisiting the social cost of carbon," *Proceedings of the National Academy of Sciences*, 2017, *114* (7), 1518–1523.

Quéré, Corinne Le, Robbie M. Andrew, Pierre Friedlingstein, Stephen Sitch, Judith Hauck, Julia Pongratz, Penelope A. Pickers, Jan Ivar Korsbakken, Glen P. Peters, Josep G. Canadell, Almut Arneth, Vivek K. Arora, Leticia Barbero, Ana Bastos, Laurent Bopp, Frédéric Chevallier, Louise P. Chini, Philippe Ciais, Scott C. Doney, Thanos Gkritzalis, Daniel S. Goll, Ian Harris, Vanessa Haverd, Forrest M. Hoffman, Mario Hoppema, Richard A. Houghton, George Hurtt, Tatiana Ilyina, Atul K. Jain, Truls Johannesen, Chris D. Jones, Etsushi Kato, Ralph F. Keeling, Kees Klein

Goldewijk, Peter Landschützer, Nathalie Lefèvre, Sebastian Lienert, Zhu Liu, Danica Lombardozzi, Nicolas Metzl, David R. Munro, Julia E. M. S. Nabel, Shin ichiro Nakaoka, Craig Neill, Are Olsen, Tsueno Ono, Prabir Patra, Anna Peregon, Wouter Peters, Philippe Peylin, Benjamin Pfeil, Denis Pierrot, Benjamin Poulter, Gregor Rehder, Laure Resplandy, Eddy Robertson, Matthias Rocher, Christian Rödenbeck, Ute Schuster, Jörg Schwinger, Roland Séférian, Ingunn Skjelvan, Tobias Steinhoff, Adrienne Sutton, Pieter P. Tans, Hanqin Tian, Bronte Tilbrook, Francesco N. Tubiello, Ingrid T. van der Laan-Luijkx, Guido R. van der Werf, Nicolas Viovy, Anthony P. Walker, Andrew J. Wiltshire, Rebecca Wright, Sönke Zaehle, and Bo Zheng, "Global Carbon Budget 2018," *Earth System Science Data*, 2018.

Revelle, Roger and Hans E Suess, "Carbon dioxide exchange between atmosphere and ocean and the question of an increase of atmospheric CO2 during the past decades," *Tellus*, 1957, *9* (1), 18–27.

Ricke, Katharine L and Ken Caldeira, "Maximum warming occurs about one decade after a carbon dioxide emission," *Environmental Research Letters*, 2014, *9* (12), 124002.

Rogelj, J, D Shindell, K Jiang, S Fifita, P Forster, V Ginzburg, C Handa, H Kheshgi, S Kobayashi, E Kriegler, L Mundaca, R Séférian, and MV Vilarino, "Mitigation pathways compatible with 1.5°C in the context of sustainable development," in V Masson-Delmotte, P Zhai, HO Pörtner, D Roberts, J Skea, PR Shukla, A Pirani, W Moufouma-Okia, C Péan, R Pidcock, S Connors, JBR Matthews, Y Chen, X Zhou, MI Gomis, E Lonnoy, T Maycock, M Tignor, and T Waterfield, eds., *Global Warming of 1.5°C. An IPCC Special Report on the impacts of global warming of 1.5°C above pre-industrial levels and related global greenhouse gas emission pathways, in the context of strengthening the global response to the threat of climate change, sustainable development, and efforts to eradicate poverty*, In Press, 2018.

Solomon, Susan, Gian-Kasper Plattner, Reto Knutti, and Pierre Friedlingstein, "Irreversible climate change due to carbon dioxide emissions," *Proceedings of the National Academy of Sciences*, 2009, *106* (6), 1704–1709.

Stern, N., *The Economics of Climate Change: the Stern Review*, Cambridge University Press, 2007.

Stocker, T.F., D. Qin, G.-K. Plattner, L.V. Alexander, S.K. Allen, N.L. Bindoff, F.-M. Bréon, J.A. Church, U. Cubasch, S. Emori, P. Forster, P. Friedlingstein, N. Gillett, J.M. Gregory, D.L. Hartmann, E. Jansen, B. Kirtman, R. Knutti, K. Krishna Kumar, P. Lemke, J. Marotzke, V. Masson-Delmotte, G.A. Meehl, I.I. Mokhov, S. Piao, V. Ramaswamy, D. Randall, M. Rhein, M. Rojas, C. Sabine, D. Shindell, L.D. Talley, D.G. Vaughan, and S.-P. Xie, "Technical Summary," in T.F. Stocker, D. Qin, G.-K. Plattner, M. Tignor, S.K. Allen, J. Boschung, A. Nauels, Y. Xia, V. Bex, and P.M. Midgley, eds., *Climate Change 2013: The Physical Science Basis. Contribution of Working Group I to the Fifth Assessment Report of the Intergovernmental Panel on Climate Change*, Cambridge, United Kingdom and New York, NY, USA: Cambridge University Press, 2013.

van der Ploeg, Frederick, "The safe carbon budget," *Climatic Change*, 2018, *147* (1-2), 47–59.

_ **and Armon Rezai**, "The agnostic's response to climate deniers: Price carbon!," *European Economic Review*, 2019, *111*, 70–84.

A Climate model experiments

Figure 1 plots the dynamic temperature responses of climate science models and economic models to an instantaneous 100GtC emission of CO_2. Each model response is a convolution of the dynamic response of the atmospheric CO_2 concentration to the 100GtC emissions pulse and the dynamic response of global mean temperature to the resulting atmospheric CO_2 concentration trajectory. The former is simulated using a carbon cycle model, the latter using a model of temperature dynamics.

The carbon-cycle response is generated by following the experimental protocol of Joos et al. (2013). The background concentration of CO_2 in the atmosphere is initialised on the observed 2010 level, i.e. 389ppm or 829GtC.[20] We assume a pre-industrial atmospheric CO_2 concentration of 275.8ppm, resulting in an excess concentration of 113.2ppm in 2010.

For each of the 16 carbon cycle models that formed part of the CMIP5 study, the four-box carbon cycle model of Joos et al. (2013) is used as a reduced-form representation. Joos et al. (2013) document the fitting procedure and resulting parameter values. The initial excess atmospheric CO_2 concentration of 113.2ppm relative to pre-industrial needs to be distributed among the four boxes of the Joos et al. model. The same need arises for the FAIR model, which shares the same four-box structure. Moreover, as the Joos et al. model was not designed to reproduce *historical* removal of CO_2 from the atmosphere (Millar et al., 2017), it is the FAIR model that we use to initialise the boxes in all of these models. To do this, we feed historical emissions into FAIR from 1890 to 2010.[21] This results in the following distribution of the initial excess concentration between the four boxes: 52.9% in box 1; 34.3% in box 2; 11.1% in box 3; 1.6% in box 4.

To keep the atmospheric CO_2 concentration constant after 2010, the experimental protocol of Joos et al. (2013) continues to add emissions. We compute these emissions as follows. The Joos et al. model implies that

$$\dot{m}_i = \psi_i E - \lambda_i m_i, \tag{10}$$

where m_i is the carbon stock in each box i, ψ_i is the proportion of emissions that enter each box and λ_i is the rate of removal of CO_2 from each box by carbon sinks. Constant atmospheric CO_2

[20] We use a conversion rate of 100GtC = 46.9ppm throughout the paper.

[21] We obtain emissions between 1890 and 1990 from the EDGAR 1.4 database and between 1990 and 2010 from the SSP database.

therefore requires

$$\sum_i \dot{m}_i = 0 \Leftrightarrow E = \sum_i \lambda_i m_i. \tag{11}$$

Substituting (11) into (10) gives a solution for decay in each box:

$$\dot{m}_j = \psi_j \left[\sum_i \lambda_i m_i \right] - \lambda_j m_j. \tag{12}$$

As time goes by, carbon is transferred from the fast-decaying boxes in the model to the permanent box and in the steady state all carbon must be in the permanent box ($i = 1$). The same emissions path is used in simulations with all the carbon cycle models considered here.

The resulting background scenario is compared to a scenario with the same emissions path, but with an impulse of 100GtC added to the atmosphere at time zero (the year 2010). The 100GtC is added to each carbon box in proportion ψ_i.

The 16 CMIP5 carbon cycle models emulated by Joos et al. (2013) are then combined with 16 CMIP5 temperature models (i.e. atmosphere-ocean general circulation models), which are represented in reduced form using the model of Geoffroy et al. (2013), as described in their paper. We set the climate sensitivity equal to 3.1°C in all models.[22] This allows us to focus on temperature inertia in the climate models. For all models, we use 0.85°C as initial atmospheric warming relative to pre-industrial in 2010. The initial lower ocean temperature is 0.22°C above pre-industrial, obtained by running FAIR on historical emissions.

FAIR is identical to the model of Joos et al. (2013), except that the residence time of CO_2 in each of the four atmospheric boxes is modified by a parameter α representing carbon cycle feedbacks. FAIR calculates α as a function of the integrated CO_2 impulse response function (iIRF) over the first 100 years of the model horizon. The assumed relationship between α and iIRF_{100} in FAIR has no analytical solution, but can be well approximated by fitting an exponential function, which results in the following solution:

$$\alpha = 0.0107 \exp\left(0.0866 \text{iIRF}_{100}\right). \tag{13}$$

[22]DICE assumes a climate sensitivity of 3.1°C. The mean climate sensitivity in Geoffroy et al. (2013) is between 3.05°C and 3.25°C, according to how models are aggregated ($\bar{\lambda} \times \overline{T_{CO_2x2}} = 3.05°C$ while $\overline{\lambda \times T_{CO_2x2}} = 3.25°C$). Default FAIR uses a climate sensitivity of 2.75°C.

We now turn to the economic models included in Figure 1. We take each of these models "off the shelf", except that, in order to be consistently compared following the experimental protocol of Joos et al. (2013), we ensure all the models are initialised on the same atmospheric carbon stock and atmospheric temperature:

- In DICE 2016, the carbon stocks are initialised on the year 2015, when the atmospheric CO_2 concentration is assumed to be 399.4ppm. Hence we reduce the excess carbon content of the three carbon boxes in DICE 2016 by 9.2% to obtain comparable 2010 initial conditions.[23] We do not change the initial deep ocean temperature in DICE 2016.

- For the PAGE and FUND models, it is most convenient to adjust the timing of the emission impulse so that the background CO_2 concentration is 389ppm – 2008 in FUND, 2009 in PAGE.

- For Golosov et al. (2014), we assume that 51.4% of the excess emissions in 2010 are in the permanent box and 48.6% are in the slow-decaying box. These numbers are obtained by using the authors' initial values in 2000 and running their model on historical emissions between 2000 and 2010.

- Gerlagh and Liski (2018) do not explicitly model temperature. CO_2 emissions map on to atmospheric concentrations and these in turn map directly on to damages. They define a common adjustment speed of temperature and damages in a one-box model. This gives $T_{t+1} = T_t - \varepsilon(ECS \times \log_2(M_t/M_{1850}) - T)$.

- For Lemoine and Rudik (2017), we can directly impute the initial atmospheric CO_2 concentration and temperature.

Figure 2 is based on a different experimental protocol. It shows yearly carbon uptake by sinks as a function of the atmospheric CO_2 concentration for constant emissions of 39.1GtCO_2 and constant non-CO_2 forcing of 0.181W/m^2, which correspond to 2015 forcing in the SSP database.[24] To make the graph, we use 2015 initial conditions, with 263GtC in the atmosphere (as in DICE) and 0.85°C

[23]The CO_2 impulse response function is independent of initial conditions and of the post-2010 emissions path in all models except FAIR, because the initial conditions and post-2010 emissions affect the background scenario and the impulse scenario (+100GtC) in the same way. The post-2010 emissions path has a small effect on temperature, however, due to the logarithmic relationship between atmospheric CO_2 and radiative forcing.

[24]Hosted by the IIASA Energy Program at https://tntcat.iiasa.ac.at/SspDb.

warming (also as in DICE). For FAIR, we use the same relative distribution among the four boxes as above and 0.28°C deep ocean warming.

Figure 3 is generated using exactly the same procedure as Figure 1, but reports the difference in atmospheric CO_2 concentration instead of the difference in temperature.

Figure 4 uses the same background scenario as Figure 1. This is compared to a scenario with a constant CO_2 concentration of 436ppm (398ppm+100GtC) from 2010 onwards.

B Further details on carbon cycle and warming models

B.1 Linear models of the carbon cycle

The linear carbon cycle is described by n difference equations, where $\mathbf{m}_t$ is a vector whose elements contain the amount of carbon in each box at time t, $\mathbf{A}$ is a square matrix of constants and $\mathbf{b}$ is a column vector. Let $\mathbf{d}$ be the vector that maps the contents of the various boxes into the stock of atmospheric carbon, i.e.

$$M_t \equiv \mathbf{d}'\mathbf{m}_t = \mathbf{d}' \left[\mathbf{A}^t M_0 + \sum_{s=1}^{t} \mathbf{A}^{t-s} \mathbf{b} E_s \right].$$

Spectral decomposition yields $\mathbf{A} = \mathbf{V}\boldsymbol{\Lambda}\mathbf{V}^{-1}$, where the diagonal matrix contains the eigenvalues in decreasing order of magnitude along its diagonal and the columns of the n x n matrix $\mathbf{V}$ contain the linearly independent eigenvectors (assuming all eigenvalues are distinct). Given that the columns of $\mathbf{A}$ must sum to one, the first of the n eigenvalues equals 1 and the others are between zero and one (provided the system is stable). Hence,

$$M_t = \mathbf{d}'\mathbf{V} \left[\boldsymbol{\Lambda}^t \mathbf{V}^{-1} M_0 + \sum_{s=1}^{t} \boldsymbol{\Lambda}^{t-s} \mathbf{V}^{-1} \mathbf{b} E_s \right].$$

The effect of a change in the emissions path from some reference path on the corresponding change in the stock of atmospheric carbon is independent of M_0 and given by

$$\Delta M_t = \mathbf{d}'\mathbf{V} \sum_{s=1}^{t} \boldsymbol{\Lambda}^{t-s} \mathbf{V}^{-1} \mathbf{b} \Delta E_s.$$

Define $\bar{\mathbf{d}} \equiv \mathbf{V}'\mathbf{d}$ and $\bar{\mathbf{b}} \equiv \mathbf{V}^{-1}\mathbf{b}$, so that

$$\Delta M_t = \sum_{s=1}^{t} \sum_{i=1}^{n} \psi_i {\lambda_i}^{t-s} \Delta E_s,$$

where $\psi_i \equiv \bar{b}_i \bar{d}_i$ are the fractions of emissions going into each of the boxes and the λ_i are the eigenvalues of the matrix $\mathbf{A}$. The impulse response function shows the effects of a small impulse in the first period only and equals $\frac{\Delta M_t}{\Delta E_1} = \sum_{i=1}^{n} \psi_i {\lambda_i}^{t-1}$. The first eigenvalue is 1 and captures that a proportion of emissions ψ_i stays in the atmosphere forever. We thus write the impulse response as the sum of its permanent and transitory components, i.e.

$$\frac{\Delta M_t}{\Delta E_1} = \psi_1 + \sum_{i=2}^{n} \psi_i {\lambda_i}^{t-1}.$$

The FUND model

The FUND carbon cycle model, which is based on Maier-Reimer and Hasselmann (1987), has 5 boxes with shares of emissions flowing into each of them equal to $\mathbf{b} = (0.13, 0.20, 0.32, 0.25, 0.1)'$, $\mathbf{d} = (1, 1, 1, 1, 1)'$ and $\mathbf{A}$ has diagonal elements equal to exp(-1/lifetime), where the lifetimes for the 5 boxes are ∞, 363, 74, 17 and 2 years respectively. These correspond to half-lives of ∞, 252, 51, 12 and 1.4 years respectively.

The Golosov et al. (2014) carbon cycle model: 2 boxes

Golosov et al. (2014) have $\mathbf{A} = \begin{pmatrix} 1 & 0 \\ 0 & 1-\varphi \end{pmatrix}$, $\mathbf{b} = \begin{pmatrix} \theta_L \\ \theta_0(1-\theta_L) \end{pmatrix}$ and $\mathbf{d} = \begin{pmatrix} 1 \\ 1 \end{pmatrix}$, where $0 < \theta_L < 1$ and $1 - \theta_L$ are the proportions of emissions that flow into the boxes holding the permanent and transitory components of atmospheric carbon respectively, $0 < \theta_0 < 1$ is the proportion of atmospheric carbon in the transitory box that decays within the span of a unit of time (i.e. within a decade), and $\varphi > 0$ denotes the speed of decay of carbon in the transitory box. Hence Eq. (3) becomes

$$M_t = m_0(1) + (1-\varphi)^t m_0(2) + \sum_{s=1}^{t} \left[\theta_L + \theta_0(1-\theta_L)(1-\varphi)^{t-s} \right] E_s,$$

where the term in square brackets shows how much of an emission impulse at time s is left in the atmosphere at time t. Roughly a fifth of carbon stays up in the atmosphere "forever", half of an emission impulse is removed after 30 years, and the remaining carbon in the atmosphere has a mean life of 300 years. This yields $\theta_L = 0.2$, $\theta_0 = 0.393$ and $\varphi = 0.0228$. It follows that the half-life equals $\ln(0.5)/\ln(0.9772) = 30$ decades. The initial values for 2010 are $S_0(1) = 684$ GtC and $S_0(2) = 118$GtC. Our starting date is 2015, so we update these and use $S_0(1) = 712$GtC and $S_0(2) = 159$GtC instead.

The DICE 2016 carbon cycle model: 3 boxes

The DICE 2016 carbon cycle of Nordhaus (2017) has three boxes: (1) the atmosphere, (2) the upper oceans and biosphere, and (3) the lower/deep oceans. The diffusion matrix is

$$\mathbf{A} = \begin{pmatrix} 0.88 & 0.196 & 0 \\ 0.12 & 0.797 & 0.001465 \\ 0 & 0.007 & 0.998535 \end{pmatrix}$$

and $\mathbf{b} = \mathbf{d} = (1, 0, 0)'$. No carbon leaves the system, so the elements of the columns of $\mathbf{A}$ sum to 1. The rate of uptake by the biosphere and oceans is independent of the amount of carbon stored in each box, so positive feedback between atmospheric CO_2 and CO_2 uptake is ruled out. There is no direct interchange of carbon between the atmosphere and the lower/deep oceans. The lower/deep oceans can store a large amount of carbon, but the rate of diffusion into the lower/deep oceans is only 0.007. The eigenvalues of $\mathbf{A}$ are (0.6796, 0.9959, 1) and

$$\mathbf{V} = \begin{pmatrix} 0.6991 & 0.5075 & 0.3173 \\ -0.7148 & 0.3002 & 0.1942 \\ 0.0157 & -0.8077 & 0.9282 \end{pmatrix},$$

so $\bar{\mathbf{b}} = (0.5283, 0.8085, 0.6946)'$, $\bar{\mathbf{d}} = (0.6991, 0.5075, 0.3173)'$ and thus the ψ_i are 37%, 41% and 22%. Since no carbon leaves the boxes, one of the eigenvalues equals 1. The smallest eigenvalue corresponds to a half-life of 9 years (5 x $\ln(0.5)/\ln(0.6796)$) and the middle one corresponds to a half-life of 851 years.

The Gerlagh and Liski (2018) carbon cycle model: 3 boxes

Gerlagh and Liski (2018) have boxes for (i) the atmosphere and the upper oceans, (ii) the biosphere and (iii) the lower oceans. Since within a decade (their unit of time) carbon mixes perfectly between the atmosphere and the upper oceans, these are combined into box one. The stock of atmospheric carbon S_t is a constant share of the contents of box one, i.e. $\mathbf{d} = (0.914, 0, 0)'$. They have

$$\mathbf{A} = \begin{pmatrix} 0.6975 & 0.2131 & 0.029 \\ 0.1961 & 0.7869 & 0 \\ 0.1063 & 0 & 0.9706 \end{pmatrix}$$

and $\mathbf{b} = (0.8809, 0.0744, 0.0447)'$. The eigenvalues of $\mathbf{A}$ are 0.5286, 0.9264 and 1, and we calculate the corresponding ψ_i to be 44.5%, 18.2% and 16.2%. The eigenvalues imply that the half-lives for the two temporary boxes are 90 and 11 years.

The Joos et al. (2013) carbon cycle model: 4 boxes

Joos et al. (2013) use a continuous-time model with one permanent and three transitory boxes to fit impulse response functions to an ensemble of Earth System model simulations.[25] They get

$$\mathbf{A} = \begin{pmatrix} 1 & 0 & 0 & 0 \\ 0 & 0.9975 & 0 & 0 \\ 0 & 0 & 0.9730 & 0 \\ 0 & 0 & 0 & 0.7927 \end{pmatrix},$$

$\mathbf{b} = \psi = (0.2173, 0.2240, 0.2824, 0.2763)'$ and $\mathbf{d} = (1, 1, 1, 1)'$ on an annual basis. The mean lags for the temporary boxes are 277, 25 and 3 years. Aengenheyster et al. (2018) also estimate a 4-box model in continuous time.

The Delay 56 and Delay 112 carbon cycle models use the same values as Joos et al. (2013) for ψ, but multiply the mean lags by five and ten respectively. In other words, any point on the impulse response function will be a point on the Delay 56 (112) impact response function five (ten) years later.

[25] In continuous time, their model is $\dot{\mathbf{m}} = \mathbf{b}E - (\mathbf{A} - \mathbf{I})\,\mathbf{m}$.

The PAGE model

The PAGE09 carbon cycle model (Hope, 2006, 2011, 2013) can be approximated using three boxes with shares of emissions flowing into each of them equal to $\mathbf{b} = (0.19, 0.43, 0.38)'$ and $\mathbf{d} = (1, 1, 0)'$, and $\mathbf{A}$ has diagonal elements equal to exp(-1/lifetime), where the lifetimes for the 3 boxes are ∞, 73.33 and close to 0 years respectively. A feedback from temperature to carbon concentration is introduced in PAGE09, which scales up the concentration from the dynamic system by a 'gain' factor to compute forcing in that year. The gain factor does not, however, influence the evolution of carbon stocks. This feedback, which models the decreasing absorptive capacity of oceans and potentially that of soil, is a linear relation of temperature (with an uncertain constant of median 9.67%/°C). However, a maximum of 53.33% can be added to the atmospheric carbon concentration.

B.2 Temperature dynamics models

In parallel to the analysis of the carbon cycle above, let temperature be given by $T_t = \mathbf{d}'\mathbf{m}_t$, where the vector $\mathbf{m}_t$ follows from the linear system $\mathbf{m}_t = \mathbf{A}\mathbf{m}_{t-1} + \mathbf{b}F_t$. Using spectral decomposition, $\mathbf{A} = \mathbf{V}\mathbf{\Lambda}\mathbf{V}^{-1}$ and defining $\bar{\mathbf{d}} \equiv \mathbf{V}'\mathbf{d}$ and $\bar{\mathbf{b}} \equiv \mathbf{V}'\mathbf{b}$, we can solve for

$$T_t = \bar{\mathbf{d}} \left(\mathbf{\Lambda}^t \mathbf{V}^{-1} T_0 + \sum_{s=1}^{t} \mathbf{\Lambda}^{t-s} \bar{\mathbf{b}} F_s \right) = \bar{\mathbf{d}}' \mathbf{\Lambda}^t \mathbf{V}^{-1} T_0 + \sum_{s=1}^{t} \sum_{i=1}^{2} \psi_i^T \lambda_i^{T\, t-s} F_s,$$

where $\psi_i^T \equiv \bar{b}_i \bar{d}_i,\ i = 1, 2$. It follows that the temperature response to a step increase in forcing, $F_s = \Delta F$, $\forall s \geq 1$, and to an increase in initial temperature equals

$$\Delta T_t = \bar{\mathbf{d}}' \mathbf{\Lambda}^t \mathbf{V}^{-1} T_0 + \left[\sum_{i=1}^{2} \frac{\psi_i^T}{(1 - \lambda_i^T)} \left(1 - \lambda_i^{T\, t} \right) \right] \Delta F.$$

Note that the effects of initial temperature and a change in forcing can be added for linear systems (called the superposition principle).

Geoffroy et al. (2013)

Geoffroy et al. (2013) have a two-box model for temperature dynamics in continuous time,

$$\dot{T} = \frac{1}{C} \left[F - \lambda T - \gamma (T - T_{LO}) \right]$$

and

$$\dot{T}_{LO} = \frac{\gamma}{C_0}(T - T_{LO}),$$

where $C = 7.3$ W yr m^{-2} K^{-1} is the effective heat capacity of the upper/mixed ocean layer, $C_0 = 106$ W yr m^{-2} K^{-1} is the effective heat capacity of the deep oceans, $\lambda = 1.13$ W m^{-2} K^{-1} and $\gamma = 0.73$ W m^{-2} K^{-1}. These are the values that best fit the multi-model mean of the CMIP5 ensemble. There is a box T representing the global mean surface temperature of the atmosphere, land and upper oceans, and a box T_{LO} representing the mean temperature of the deep oceans. Steady-state temperature corresponding to constant forcing F is $T = T_{LO} = F/\lambda$, which gives an equilibrium climate sensitivity or ECS (i.e. the steady-state increase in temperature resulting from doubling the atmospheric stock of CO_2 relative to pre-industrial) of $F_{2\times CO_2}/\lambda$= 3.45/1.13 = 3.05 K given $F_{2\times CO_2} = 3.45$ W m^{-2}. To get an ECS of 3.1, we adjust by multiplying $F_{2\times CO_2}$ by the factor 3.1/3.05 and modify the first equation to $\dot{T} = \frac{1}{C}\left[(3.1/3.05)F - \lambda T - \gamma(T - T_{LO})\right]$.

The state transition matrix $\mathbf{A} = \begin{pmatrix} -(\lambda+\gamma)/C & \gamma/C \\ \gamma/C_0 & -\gamma/C_0 \end{pmatrix}$, which has eigenvalues -0.2575 and -0.0041. Using $\mathbf{d} = (1,0)'$ and $\mathbf{b} = (1/C, 0)'$, we obtain $\psi_1^T = 0.135$ and $\psi_2^T = 0.0015$, which gives the following impulse response function:

$$\frac{\Delta T(t)}{\Delta F(s)} = 0.135\exp(-0.2575(t-s)) + 0.0015\exp(-0.0041(t-s)).$$

Notice ψ_1^T is much larger than ψ_2^T, i.e. the system responds quickly to an impulse of forcing. Since the lower ocean has a large heat capacity, it quickly absorbs the extra heat in the atmosphere.

By contrast, the reaction to a step increase in forcing ΔF is slower. The temperature increase for a step increase in forcing beginning at time s, with a steady-state temperature effect of $\Delta F/\lambda$, is

$$\frac{\Delta T(t)}{\Delta F} = \frac{1}{\lambda}\left[1 - 0.523\exp(-0.2575(t-s)) - 0.366\exp(-0.0041(t-s))\right].$$

This formula is based on the same eigenvalues, but the relative weight on the slow box is much larger: $\hat{\psi}_1^T = 0.523$ versus $\hat{\psi}_2^T = 0.366$. With constant forcing, the deep ocean reaches the same steady-state temperature as the atmosphere, but, given the large heat capacity of the deep ocean, it takes much longer to reach.

For the Delay 56 and Delay 112 model versions, we multiply the capacities C and C_0 by factors of 5 and 10 respectively. This does not affect the values of ψ_i^T. However, the Delay 56 system has eigenvalues of -0.0515 and -0.0008; the Delay 112 system -0.0258 and -0.0004. In other words, half-lives are multiplied by 5 and 10 for the Delay 56 and Delay 112 variants respectively.

DICE 2016

DICE 2016 is formulated in discrete time with a time unit of 5 years and, like the model of Geoffroy et al. (2013), has two heat boxes, one for the temperature of the atmosphere, land and upper oceans, and one for the temperature of the deep oceans:

$$T_t = T_{t-1} + \frac{1}{C_{UP}}\left[F_t - \frac{3.6813}{ECS}T_{t-1} - 0.088(T_{t-1} - T_{LO,t-1})\right]$$

and

$$T_{LO,t} = T_{LO,t-1} + \frac{0.088}{C_{LO}}(T_{t-1} - T_{LO,t-1}),$$

where $C_{UP} = 1/0.1005$ W yr m^{-2} K^{-1} and $C_{LO} = 0.088/0.025$ W yr m^{-2} K^{-1} are the effective heat capacities of the upper and lower oceans respectively, and 0.088 and 0.025 are the coefficients of heat exchange between the upper and deep oceans respectively. The steady state temperature is $T_t = T_{LO,t} = ECS \times F_t/3.6813 = 0.842F_t$, where ECS is set to 3.1 K. The transient climate sensitivity is set to 1.7 K. The transition matrix $\mathbf{A} = \begin{pmatrix} 0.873 & 0.009 \\ 0.025 & 0.975 \end{pmatrix}$, $\mathbf{b} = (1/C_{UP}, 0)'$ and $\mathbf{d} = (1, 0)'$. This yields eigenvalues 0.871 and 0.977 with corresponding shares $\psi_1^T = 0.0985$ and $\psi_2^T = 0.002$. Note that $\psi_1^T + \psi_2^T = 1/C_{UP} = 0.1005$. The temperature response to an impulse in forcing is $\frac{\Delta T_t}{\Delta F_1} = 0.0985 \times 0.8711^{t-1} + 0.0022 \times 0.9771^{t-1}$. The temperature response to a step increase in forcing at time s equals

$$\frac{\Delta T_t}{\Delta F} = \sum_{i=1}^{2}\left(\frac{\psi_i^T \lambda_i^{T\,t}}{1 - \lambda_i^{T\,t}}\right) = \frac{0.0985 \times (1 - 0.871^t)}{0.129} + \frac{0.002 \times (1 - 0.977^t)}{0.003}.$$

We find that $\lim_{t\to\infty} \frac{\Delta T_t}{\Delta F} = \sum_{i=1}^{2} \frac{\psi_i^T}{\lambda_i^T} \to \frac{0.0985}{0.129} + \frac{0.002}{0.003} = 0.8521.$

Golosov et al. (2014)

Golosov et al. (2014) have no temperature lag, so they have $T_t = 0.842F_t$.

Gerlagh and Liski (2018)

Gerlagh and Liski (2018) have a simple lag with partial adjustment of 0.183 per decade (or 2% per year), so they have

$$T_t = T_{t-1} + 0.183\ (0.842F_t - T_{t-1}).$$

This corresponds to a half-life of 34 years. Although this long lag is in line with the scientific evidence of some time ago (Solomon et al., 2009), it does not accord with more recent scientific evidence (e.g Geoffroy et al., 2013). The resulting temperature response to an impulse in forcing is $\frac{\Delta T_t}{\Delta F_1} = 0.842 \times 0.817^{t-1}$. The corresponding response to a step increase in forcing is

$$\frac{\Delta T_t}{\Delta F} = 0.842 \times \frac{1 - 0.817^t}{0.183}.$$

FUND

The annual FUND model also has a simple temperature lag, but with a partial adjustment coefficient of 0.0224 per year, corresponding to a mean lag of 44.6 years and a half-life of 30.6 years.

PAGE

Global mean temperature in PAGE09 is the weighted sum of regional temperatures. Once aggregated, however, global temperature follows a median life-time of 24 years (and mean of 50 years).

Convoluted temperature response function

Equation (9) gives the convoluted temperature response function, which is derived from the carbon stock-emissions response function, the temperature-forcing response function, and $\frac{\partial T_s}{\partial S_s} = \frac{F_{2\times CO_2}}{\ln 2} \frac{1}{M_s}$. The temperature response to a small step change in the stock of atmospheric carbon, $\Delta S_s = \Delta S,\ \forall S \geq 0$, is thus $\frac{\Delta T_t}{\Delta S} = \frac{F_{2\times CO_2}}{\ln 2} \frac{1}{M_0} \frac{\Delta T_t}{\Delta F}$ for the Geoffroy et al. (2013) model and $\frac{\Delta T_t}{\Delta S} = \frac{F_{2\times CO_2}}{\ln 2} \frac{1}{M_1} \frac{\Delta T_t}{\Delta F}$ for the discrete-time models such as DICE. Note that the response to a step increase in atmospheric carbon decreases in the values of the atmospheric carbon stock. To calculate these convoluted step responses, we suppose that the concentration of atmospheric carbon stays constant at its initial value. Hence, we set M_s to 3038 GtCO2 or 389 ppmv for all s. For the DICE model we thus get $\frac{\Delta T_t}{\Delta S} = \frac{F_{2\times CO_2}}{\ln 2}\frac{1}{M_1}\frac{\Delta T_t}{\Delta F} = 0.0012585$ as $t \to \infty$. For a small step change in atmospheric carbon of 100 GtC, the steady-state increase in temperature would then equal $0.0012585 \times 100 \times 44/12 = 0.46$ K, which is consistent with the plot in Figure 4.

C Further results

DICE 2016 compared with DICE-FAIR-Geoffroy

Here we compare standard DICE 2016 (row 5) with DICE-FAIR-Geoffroy (row 1). This comparison is affected by differences in: (a) temperature dynamics between the DICE 2016 and Geoffroy et al. (2013) models; (b) removal of atmospheric CO_2 between the DICE 2016 and Joos et al. (2013) carbon cycles, and; (c) assumptions about (non-)diminishing marginal removal of atmospheric CO_2 between DICE 2016/Joos et al. (2013) and FAIR. Therefore this comparison is of the combined effect of all the modifications to DICE that we have identified, which would bring it fully into line with the climate science models we have assembled.

The combined effect of these is a higher optimal carbon price in DICE 2016 than in DICE-FAIR-Geoffroy (see Figure 5). The 2020 optimal carbon price is 24% higher in DICE 2016. Yet it is on the 2°C cost-minimising paths that we see the largest price differences. The 2020 2°C cost-minimising carbon price is three times higher in DICE 2016 than in DICE-FAIR-Geoffroy, resulting in a reduction in 2020 emissions of almost 9GtCO_2. Yet, despite lower emissions throughout this century on both the optimal and 2°C cost-minimising paths, temperatures end up being higher in DICE 2016, by more than 0.5°C in 2100 on the optimal path. The main driver of these differences is the tendency of DICE 2016 to heat up too much in the long run, as the analysis just below will show. This is particularly manifest on the 2°C cost-minimising path, because heating up too much in the long run makes it extremely difficult to avoid the global mean temperature exceeding 2°C above the pre-industrial level.

A method of apportioning the differences between DICE 2016 and DICE-FAIR-Geoffroy to factors (a) to (c) is to plot the percentage difference in carbon prices and temperatures – always relative to DICE-FAIR-Geoffroy – in DICE 2016, DICE-Geoffroy (i.e. combining the DICE 2016 carbon cycle with the Geoffroy et al. (2013) temperature dynamics model), DICE-Joos (i.e. combining the Joos et al. (2013) carbon cycle with the DICE 2016 temperature dynamics model) and DICE-Joos-Geoffroy. Figure 6 does this.[26] The way to intuit this figure is that whichever model is closest to DICE 2016 explains most of the difference between it and DICE-FAIR-Geoffroy. Hence the main contributing factor to the difference in *optimal* carbon prices between DICE 2016 and DICE-FAIR-Geoffroy is (b) insufficient removal of atmospheric CO_2 in DICE 2016 (top left panel). This is a feature shared by DICE 2016 and DICE-Geoffroy, but not by the other models, which incorporate the four-box carbon cycle of Joos et al. (2013). However, when it comes to the 2°C carbon price, or temperature on either path, the main contributing factor to the difference between DICE 2016 and DICE-FAIR-Geoffroy is (a) temperature dynamics. Excessive delay, offset by excessive long-term warming, is a feature shared by the DICE 2016 and DICE-Joos variants. Excessive delay and excessive long-term warming are responsible for the temperature trajectories in DICE 2016 that start below DICE-FAIR-Geoffroy but end up higher, significantly so on the optimal path. Excessive long-term warming also explains the high 2°C carbon price, because it significantly limits the 2°C carbon budget.

[26] For this comparison we omit emissions, because when emissions approach or reach zero the differences between the models can explode or be undefined respectively.

Figure 6: Price and temperature paths relative to the benchmark DICE-FAIR-Geoffroy model. Left column – welfare-maximising path; right column – cost-effective path to limit warming to 2°C. Top row – carbon prices; bottom row – warming. Whichever model is closest to DICE 2016 explains most of the difference between it and DICE-FAIR-Geoffroy.

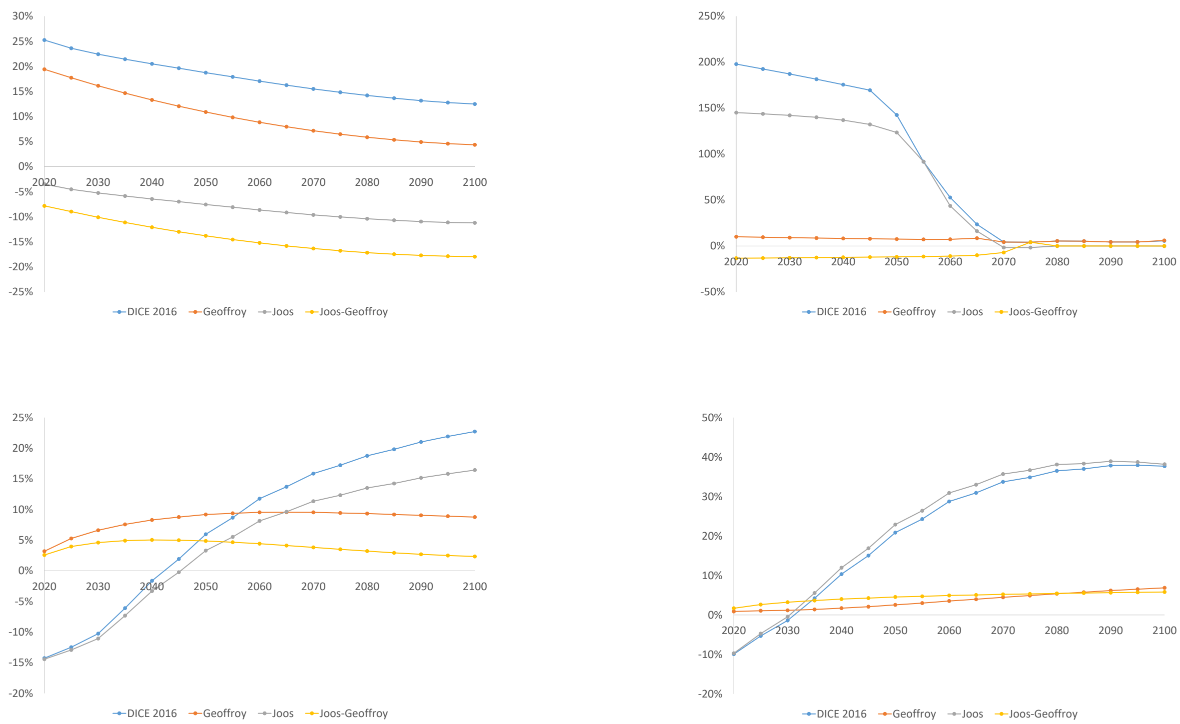

2°C cost minimisation under different exogenous emissions/forcing scenarios

Figure 7 shows using DICE-FAIR-Geoffroy that limiting warming to 2°C is much more costly when exogenous CO_2 emissions/forcing come from standard DICE 2016 than when they come from the IPCC's RCP2.6 scenario. The former scenario was designed to apply no matter the amount of CO_2 emissions abatement undertaken in the model (i.e. from the energy sector), while the latter was designed by IPCC to imply a level of abatement outside CO_2/energy that is consistent with the 2°C goal. Limiting warming to 2°C is infeasible in DICE 2016 with standard DICE 2016 exogenous emissions/forcing.

Figure 7: 2°C cost-minimising carbon prices in DICE-FAIR-Geoffroy using two alternative scenarios for emissions of CO_2 from land use and forestry, and exogenous radiative forcing from other greenhouse gases and agents. Carbon prices are much higher under the standard DICE 2016 scenario than under the RCP2.6 scenario.

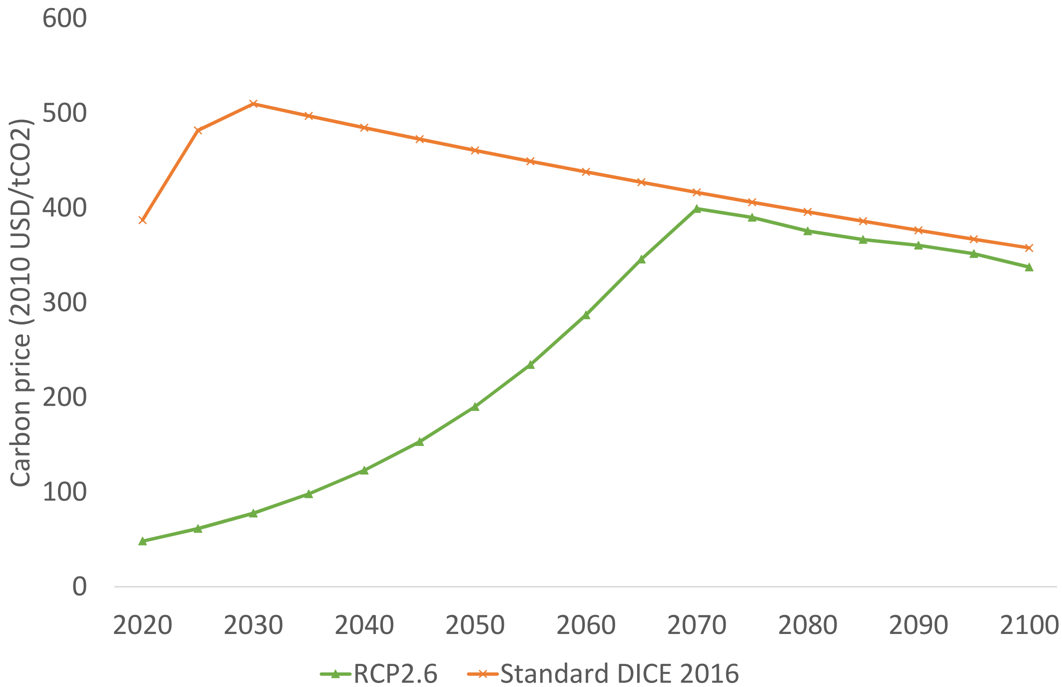

D GAMS code for DICE 2016 with the FAIR carbon cycle and the Geoffroy et al. (2013) temperature model

In this section we provide GAMS code to implement the FAIR carbon cycle in DICE 2016, as well as parameters to implement the Geoffroy et al. (2013) warming model. This replaces the three-box model of the carbon cycle and the two-box temperature model of standard DICE 2016.

```
$ontext
This is a modified version of DICE-2016R-091916ap.gms.
The carbon cycle has been changed to the four box model of Joos et al. and parameters of thermal
dynamics to match Geoffroy et al. The positive feedback from sink satiation has been added. See
**-comments for details throughout.

$title        DICE-2016R September 2016 (DICE-2016R-091216a.gms)
$offtext

set        t  Time periods (5 years per period)                    /1*100/

PARAMETERS
** Availability of fossil fuels
        fosslim  Maximum cumulative extraction fossil fuels (GtC)  /6000/
**Time Step
        tstep    Years per Period                                  /5/
** If optimal control
        ifopt    Indicator where optimized is 1 and base is 0      /0/
        ifmiulim Indicator where fixed miu('1') is 1 and 0 else    /1/
** Preferences
        elasmu   Elasticity of marginal utility of consumption     /1.45 /
        prstp    Initial rate of social time preference per year   /.015  /
**new parameters for public decision making
        elasmu_pub   Elasticity of marginal utility of consumption     /1.45 /
        prstp_pub    Initial rate of social time preference per year   /.015  /

** Population and technology
        gama     Capital elasticity in production function        /.300    /
        pop0     Initial world population 2015 (millions)         /7403    /
        popadj   Growth rate to calibrate to 2050 pop projection  /0.134   /
        popasym  Asymptotic population (millions)                 /11500   /
        dk       Depreciation rate on capital (per year)          /.100    /
        q0       Initial world gross output 2015 (trill 2010 USD) /105.5   /
        k0       Initial capital value 2015 (trill 2010 USD)      /223     /
        a0       Initial level of total factor productivity       /5.115    /
        ga0      Initial growth rate for TFP per 5 years          /0.076   /
        dela     Decline rate of TFP per 5 years                  /0.005   /
** Emissions parameters
        gsigma1  Initial growth of sigma (per year)                   /-0.0152 /
        dsig     Decline rate of decarbonization (per period)         /-0.001  /
        eland0   Carbon emissions from land 2015 (GtCO2 per year)     / 2.6    /
        deland   Decline rate of land emissions (per period)          / .115   /
        e0       Industrial emissions 2015 (GtCO2 per year)           /35.85    /
        miu0     Initial emissions control rate for base case 2015    /.03     /
** Carbon cycle
** new carbon cycle replaces DICE's oceanic carbon reservoirs with four atmospheric carbon
boxes. Transition matrix is diagonal since it is a reduced-form model.
$ontext
* Initial Conditions
        mat0   Initial Concentration in atmosphere 2015 (GtC)        /851    /
        mu0    Initial Concentration in upper strata 2015 (GtC)      /460    /
        ml0    Initial Concentration in lower strata 2015 (GtC)      /1740   /
        mateq  Equilibrium concentration atmosphere  (GtC)           /588    /
        mueq   Equilibrium concentration in upper strata (GtC)       /360    /
        mleq   Equilibrium concentration in lower strata (GtC)       /1720   /
* Flow paramaters
        b12      Carbon cycle transition matrix                      /.12   /
        b23      Carbon cycle transition matrix                      /0.007 /
* These are for declaration and are defined later
        b11      Carbon cycle transition matrix
        b21      Carbon cycle transition matrix
        b22      Carbon cycle transition matrix
        b32      Carbon cycle transition matrix
        b33      Carbon cycle transition matrix
$offtext
        mperm0 Initial stock in fastes carbon box (GtC)              /139.1 /
        mslow0 Initial stock in fastes carbon box (GtC)              /90.2  /
        mmedium0 Initial stock in fastes carbon box (GtC)            /29.2  /
        mfast0 Initial stock in fastes carbon box (GtC)              /4.2   /
        b10      proportion of emissions in permanent box            /.217   /
        b11      proportion of emissions in slowes box               /.224   /
        b12      proportion of emissions in medium box               /.282   /
        b13      proportion of emissions in fast box                 /.276   /
        b21      Decay speed slowest box                             /.00254 /
        b22      Decay speed medium box                              /.0274  /
        b23      Decay speed fast box                                /.232342 /
** The follow three parameters are needed for positive feedback.
        R0       pre-industrial iIRF                                 / 34.4   /
```

```
        RC       iIRF response to CACC(GtC)                           / 0.019  /
        RT       iIRF response to T(°C)                               / 4.165  /
** End of changes.
        sig0     Carbon intensity 2010 (kgCO2 per output 2005 USD 2010)
** Climate model parameters
        t2xco2   Equilibrium temp impact (oC per doubling CO2)    / 3.1  /
        fex0     2015 forcings of non-CO2 GHG (Wm-2)              / 0.5  /
        fex1     2100 forcings of non-CO2 GHG (Wm-2)              / 1.0  /
        tocean0  Initial lower stratum temp change (C from 1900)  /.0068 /
        tatm0    Initial atmospheric temp change (C from 1900)    /0.85  /
        c1       Climate equation coefficient for upper level     /0.1005  /
        c3       Transfer coefficient upper to lower stratum      /0.088   /
        c4       Transfer coefficient for lower level             /0.025   /
        fco22x   Forcings of equilibrium CO2 doubling (Wm-2)      /3.6813  /
** Climate damage parameters
        a10       Initial damage intercept                         /0       /
        a20       Initial damage quadratic term
        a1        Damage intercept                                 /0       /
        a2        Damage quadratic term                            /0.00236 /
        a3        Damage exponent                                  /2.00    /
** Abatement cost
        expcost2  Exponent of control cost function               / 2.6  /
        pback     Cost of backstop 2010$ per tCO2 2015            / 550  /
        gback     Initial cost decline backstop cost per period   / .025 /
        limmiu    Upper limit on control rate after 2150          / 1.2 /
        tnopol    Period before which no emissions controls base  / 45   /
        cprice0   Initial base carbon price (2010$ per tCO2)      / 2    /
        gcprice   Growth rate of base carbon price per year       /.02   /

** Scaling and inessential parameters
* Note that these are unnecessary for the calculations
* They ensure that MU of first period's consumption =1 and PV cons = PV utilty
        scale1      Multiplicative scaling coefficient           /0.0302455265681763 /
        scale2      Additive scaling coefficient                 /-10993.704/ ;

* Program control variables
sets     tfirst(t), tlast(t), tearly(t), tlate(t);

PARAMETERS
        l(t)          Level of population and labor
        al(t)         Level of total factor productivity
        sigma(t)      CO2-equivalent-emissions output ratio
        rr(t)         Average utility social discount rate
        ga(t)         Growth rate of productivity from
        forcoth(t)    Exogenous forcing for other greenhouse gases
        gl(t)         Growth rate of labor
        gcost1        Growth of cost factor
        gsig(t)       Change in sigma (cumulative improvement of energy efficiency)
        etree(t)      Emissions from deforestation
        cumetree(t)   Cumulative from land
        cost1(t)      Adjusted cost for backstop
        lam           Climate model parameter
        gfacpop(t)    Growth factor population
        pbacktime(t)  Backstop price
        optlrsav      Optimal long-run savings rate used for transversality
        scc(t)        Social cost of carbon
        cpricebase(t) Carbon price in base case
        photel(t)     Carbon Price under no damages (Hotelling rent condition)
        ppm(t)        Atmospheric concentrations parts per million
        atfrac(t)     Atmospheric share since 1850
        atfrac2010(t)     Atmospheric share since 2010 ;
* Program control definitions
        tfirst(t) = yes$(t.val eq 1);
        tlast(t)  = yes$(t.val eq card(t));
* Parameters for long-run consistency of carbon cycle
** These calculations specify DICE's transition matrix in carbon cycle. They are not needed
anymore.
$ontext
        b11 = 1 - b12;
        b21 = b12*MATEQ/MUEQ;
        b22 = 1 - b21 - b23;
        b32 = b23*mueq/mleq;
        b33 = 1 - b32 ;
$offtext
** End of changes
* Further definitions of parameters
        a20 = a2;
        sig0 = e0/(q0*(1-miu0));
```

```
        lam = fco22x/ t2xco2;
        l("1") = pop0;
        loop(t, l(t+1)=l(t););
        loop(t, l(t+1)=l(t)*(popasym/L(t))**popadj ;);

        ga(t)=ga0*exp(-dela*5*((t.val-1)));
        al("1") = a0; loop(t, al(t+1)=al(t)/((1-ga(t))););
        gsig("1")=gsigma1; loop(t,gsig(t+1)=gsig(t)*((1+dsig)**tstep) ;);
        sigma("1")=sig0;   loop(t,sigma(t+1)=(sigma(t)*exp(gsig(t)*tstep)););

        pbacktime(t)=pback*(1-gback)**(t.val-1);
        cost1(t) = pbacktime(t)*sigma(t)/expcost2/1000;

        etree(t) = eland0*(1-deland)**(t.val-1);
        cumetree("1")= 100; loop(t,cumetree(t+1)=cumetree(t)+etree(t)*(5/3.666););

        rr(t) = 1/((1+prstp_pub)**(tstep*(t.val-1)));
        forcoth(t) = fex0+ (1/17)*(fex1-fex0)*(t.val-1)$(t.val lt 18)+ (fex1-fex0)$(t.val ge
18);
        optlrsav = (dk + .004)/(dk + .004*elasmu + prstp)*gama;

*Base Case Carbon Price
        cpricebase(t)= cprice0*(1+gcprice)**(5*(t.val-1));

VARIABLES
        MIU(t)          Emission control rate GHGs
        FORC(t)         Increase in radiative forcing (watts per m2 from 1900)
        TATM(t)         Increase temperature of atmosphere (degrees C from 1900)
        TOCEAN(t)       Increase temperatureof lower oceans (degrees C from 1900)
        MAT(t)          Carbon concentration increase in atmosphere (GtC from 1750)
** Old variables are moved and new ones introduced below
$ontext
        MU(t)           Carbon concentration increase in shallow oceans (GtC from 1750)
        ML(t)           Carbon concentration increase in lower oceans (GtC from 1750)
$offtext
        MPERM(t)        Carbon concentration increase in permanent box (GtC from 1750)
        MSLOW(t)        Carbon concentration increase in slow decay box (GtC from 1750)
        MMEDIUM(t)      Carbon concentration increase in medium decay box (GtC from 1750)
        MFAST(t)        Carbon concentration increase in fast decay box (GtC from 1750)
        CACC(t)         Carbon accumulated minus past satiation (GtC)
        iIRF(T)         100-year integrated impulse response function
        alpha(T)        time constant scaling factor (positive feed-back from emissions to
reduced carbon decay)
** End of changes
        E(t)            Total CO2 emissions (GtCO2 per year)
        EIND(t)         Industrial emissions (GtCO2 per year)
        C(t)            Consumption (trillions 2005 US dollars per year)
        K(t)            Capital stock (trillions 2005 US dollars)
        CPC(t)          Per capita consumption (thousands 2005 USD per year)
        I(t)            Investment (trillions 2005 USD per year)
        S(t)            Gross savings rate as fraction of gross world product
        RI(t)           Real interest rate (per annum)
        Y(t)            Gross world product net of abatement and damages (trillions 2005 USD per
year)
        YGROSS(t)       Gross world product GROSS of abatement and damages (trillions 2005 USD
per year)
        YNET(t)         Output net of damages equation (trillions 2005 USD per year)
        DAMAGES(t)      Damages (trillions 2005 USD per year)
        DAMFRAC(t)      Damages as fraction of gross output
        ABATECOST(t)    Cost of emissions reductions  (trillions 2005 USD per year)
        MCABATE(t)      Marginal cost of abatement (2005$ per ton CO2)
        CCA(t)          Cumulative industrial carbon emissions (GTC)
        CCATOT(t)       Total carbon emissions (GtC)
        PERIODU(t)      One period utility function
        CPRICE(t)       Carbon price (2005$ per ton of CO2)
        CEMUTOTPER(t)   Period utility
        UTILITY         Welfare function;

** Obsolete variables MU and ML have been removed in the declaration of non-negative variables
below. Additional ones are introduced to reflect new carbon dynamics.
* NONNEGATIVE VARIABLES  MIU, TATM, MAT, MU, ML, Y, YGROSS, C, K, I;
NONNEGATIVE VARIABLES  MIU, TATM, MAT, Y, YGROSS, C, K, I;
NONNEGATIVE VARIABLES  MPERM, MSLOW, MMEDIUM, MFAST, alpha;

EQUATIONS
*Emissions and Damages
        EEQ(t)           Emissions equation
        EINDEQ(t)        Industrial emissions
```

```
        CCACCA(t)        Cumulative industrial carbon emissions
        CCATOTEQ(t)        Cumulative total carbon emissions
        FORCE(t)         Radiative forcing equation
        DAMFRACEQ(t)     Equation for damage fraction
        DAMEQ(t)         Damage equation
        ABATEEQ(t)       Cost of emissions reductions equation
        MCABATEEQ(t)     Equation for MC abatement
        CARBPRICEEQ(t)   Carbon price equation from abatement

*Climate and carbon cycle
        MMAT(t)          Atmospheric concentration equation
** Old carbon cycle equations are removed and new equations for carbon boxes and accounting for
past sink satiation introduced.
$ontext
        MMU(t)           Shallow ocean concentration
        MML(t)           Lower ocean concentration
$offtext
        MMPERM(t)        Permanent carbon box
        MMSLOW(t)        Slow decay carbon box
        MMMEDIUM(t)      Medium decay speed carbon box
        MMFAST(t)        Fast decay carbon box
        CACCEQ(t)        Cumulative carbon emissions(t)
        iIRFeq1(t)       calibraton of IRF to 100 year impulse
        iIRFeq2(t)
** End of changes
        TATMEQ(t)        Temperature-climate equation for atmosphere
        TOCEANEQ(t)      Temperature-climate equation for lower oceans

*Economic variables
        YGROSSEQ(t)      Output gross equation
        YNETEQ(t)        Output net of damages equation
        YY(t)            Output net equation
        CC(t)            Consumption equation
        CPCE(t)          Per capita consumption definition
        SEQ(t)           Savings rate equation
        KK(t)            Capital balance equation
        RIEQ(t)          Interest rate equation

* Utility
        CEMUTOTPEREQ(t)  Period utility
        PERIODUEQ(t)     Instantaneous utility function equation
        UTIL             Objective function      ;

** Equations of the model
*Emissions and Damages
 eeq(t)..            E(t)           =E= EIND(t) + etree(t);
 eindeq(t)..         EIND(t)        =E= sigma(t) * YGROSS(t) * (1-(MIU(t)));
 ccacca(t+1)..       CCA(t+1)       =E= CCA(t)+ EIND(t)*5/3.666;
 ccatoteq(t)..       CCATOT(t)      =E= CCA(t)+cumetree(t);
 force(t)..          FORC(t)        =E= fco22x * ((log((MAT(t)/588.000))/log(2))) + forcoth(t);
 damfraceq(t) ..     DAMFRAC(t)     =E= (a1*TATM(t))+(a2*TATM(t)**a3) ;
 dameq(t)..          DAMAGES(t)     =E= YGROSS(t) * DAMFRAC(t);
 abateeq(t)..        ABATECOST(t)   =E= YGROSS(t) * cost1(t) * (MIU(t)**expcost2);
 mcabateeq(t)..      MCABATE(t)     =E= pbacktime(t) * MIU(t)**(expcost2-1);
 carbpriceeq(t)..    CPRICE(t)      =E= pbacktime(t) * (MIU(t))**(expcost2-1);

*Climate and carbon cycle
** New carbon cycle removes old equations and introduces new equations for carbon boxes,
cumulative emissions, and saturation of sinks
$ontext
 mmat(t+1)..         MAT(t+1)       =E= MAT(t)*b11 + MU(t)*b21 + (E(t)*(5/3.666));
 mml(t+1)..          ML(t+1)        =E= ML(t)*b33  + MU(t)*b23;
 mmu(t+1)..          MU(t+1)        =E= MAT(t)*b12 + MU(t)*b22 + ML(t)*b32;
$offtext
 mmat(t)..           MAT(t)         =E= MPERM(t) + MSLOW(t) + MMEDIUM(t) +  MFAST(t) + 588  ;
 mmperm(t+1)..       MPERM(t+1)     =E= b10*5/3.666 * E(t) + MPERM(t) ;
 mmslow(t+1)..       MSLOW(t+1)     =E= b11/(b21/alpha(t)) *(1-exp(-b21/alpha(t)*5))/3.666 *
E(t) + exp(-b21/alpha(t)*5)*MSLOW(t) ;
 mmmedium(t+1)..     MMEDIUM(t+1)   =E= b12/(b22/alpha(t)) *(1-exp(-b22/alpha(t)*5))/3.666 *
E(t) + exp(-b22/alpha(t)*5)*MMEDIUM(t) ;
 mmfast(t+1)..       MFAST(t+1)     =E= b13/(b23/alpha(t)) *(1-exp(-b23/alpha(t)*5))/3.666 *
E(t) + exp(-b23/alpha(t)*5)*MFAST(t) ;
 cacceq(t)..         CACC(t)        =E= CCA(t) + cumetree(t) - (MAT(T) - 588) ;
 iIRFeq1(T)..        iIRF(T)        =E= R0 + RC*CACC(T) + RT*TATM(T) ;
 iIRFeq2(T)..        iIRF(T)        =E= b10 * 100 + alpha(t) * (
                                        + b11 / b21 * ( 1 - exp( -100*b21/alpha(t) ) )
                                        + b12 / b22 * ( 1 - exp( -100*b22/alpha(t) ) )
                                        + b13 / b23 * ( 1 - exp( -100*b23/alpha(t) ) )   );
```

```
** End of changes
 tatmeq(t+1)..        TATM(t+1)      =E= TATM(t) + c1 * ((FORC(t+1)-(fco22x/t2xco2)*TATM(t))-
(c3*(TATM(t)-TOCEAN(t))));
 toceaneq(t+1)..      TOCEAN(t+1)    =E= TOCEAN(t) + c4*(TATM(t)-TOCEAN(t));

*Economic variables
 ygrosseq(t)..        YGROSS(t)      =E= (al(t)*(L(t)/1000)**(1-GAMA))*(K(t)**GAMA);
 yneteq(t)..          YNET(t)        =E= YGROSS(t)*(1-damfrac(t));
 yy(t)..              Y(t)           =E= YNET(t) - ABATECOST(t);
 cc(t)..              C(t)           =E= Y(t) - I(t);
 cpce(t)..            CPC(t)         =E= 1000 * C(t) / L(t);
 seq(t)..             I(t)           =E= S(t) * Y(t);
 kk(t+1)..            K(t+1)         =L= (1-dk)**tstep * K(t) + tstep * I(t);
 rieq(t+1)..          RI(t)          =E= (1+prstp_pub) * (CPC(t+1)/CPC(t))**(elasmu_pub/tstep) -
1;

*Utility
 cemutotpereq(t)..    CEMUTOTPER(t)  =E= PERIODU(t) * L(t) * rr(t);
 periodueq(t)..       PERIODU(t)     =E= ((C(T)*1000/L(T))**(1-elasmu_pub)-1)/(1-elasmu_pub)-1;
 util..               UTILITY        =E= tstep * scale1 * sum(t,  CEMUTOTPER(t)) + scale2 ;

*Resource limit
CCA.up(t)       = fosslim;

* Control rate limits
MIU.up(t)            = limmiu;
MIU.up(t)$(t.val<30) = 1;

**  Upper and lower bounds for stability
K.LO(t)         = 1;
MAT.LO(t)       = 10;
** following two bounds are obsolete
*MU.LO(t)        = 100;
*ML.LO(t)        = 1000;
C.LO(t)         = 2;
TOCEAN.UP(t)    = 20;
TOCEAN.LO(t)    = -1;
TATM.UP(t)      = 20;
CPC.LO(t)       = .01;
TATM.UP(t)      = 12;

* Control variables
set lag10(t) ;
lag10(t) =  yes$(t.val gt card(t)-10);
S.FX(lag10(t)) = optlrsav;

* Initial conditions
CCA.FX(tfirst)    = 400;
K.FX(tfirst)      = k0;
** following three initial conditions are obsolete and new ones introduced.
*MAT.FX(tfirst)    = mat0;
*MU.FX(tfirst)     = mu0;
*ML.FX(tfirst)     = ml0;
MPERM.FX(tfirst)    = MPERM0;
MSLOW.FX(tfirst)    = MSLOW0;
MMEDIUM.FX(tfirst)  = MMEDIUM0;
MFAST.FX(tfirst)    = MFAST0;
** End of Changes
TATM.FX(tfirst)   = tatm0;
TOCEAN.FX(tfirst) = tocean0;

** Solution options
option iterlim = 99900;
option reslim = 99999;
option solprint = on;
option limrow = 0;
option limcol = 0;
model  CO2 /all/;

** Variables changed to match thermal warming of Geoffroy et al.
c1  = 0.386 ;
lam = 1.13  ;
c3  = 0.73  ;
c4  = 0.034 ;
fco22x = 3.503;
alpha.lo(t) = .1;
alpha.up(t) = 1000;
** Exogenous forcing components (variables etree and forcoth) are adapted to SSP1 2.6.
```

```
Parameter etree_DICE, forcoth_DICE;
etree_DICE(T)  = etree(T);
forcoth_DICE(T)= forcoth(T);
Parameter etree_SSP1_26, forcoth_SSP1_26;

forcoth_SSP1_26(T)               =  0.297 ;
forcoth_SSP1_26(T)$(T.val GE 2) =  0.393 ;
forcoth_SSP1_26(T)$(T.val GE 4) =  0.497 ;
forcoth_SSP1_26(T)$(T.val GE 6) =  0.468 ;
forcoth_SSP1_26(T)$(T.val GE 8) =  0.402 ;
forcoth_SSP1_26(T)$(T.val GE 10)=  0.342 ;
forcoth_SSP1_26(T)$(T.val GE 12)=  0.302 ;
forcoth_SSP1_26(T)$(T.val GE 14)=  0.274 ;
forcoth_SSP1_26(T)$(T.val GE 16)=  0.255 ;
forcoth_SSP1_26(T)$(T.val GE 18)=  0.257 ;

etree_SSP1_26(T)              =  3517.440/1000;
etree_SSP1_26(T)$(T.val GE 2) =  3178.329/1000;
etree_SSP1_26(T)$(T.val GE 4) =   188.063/1000;
etree_SSP1_26(T)$(T.val GE 6) = - 387.799/1000;
etree_SSP1_26(T)$(T.val GE 8) = -1758.623/1000;
etree_SSP1_26(T)$(T.val GE 10)= -2586.615/1000;
etree_SSP1_26(T)$(T.val GE 12)= -2583.968/1000;
etree_SSP1_26(T)$(T.val GE 14)= -2436.902/1000;
etree_SSP1_26(T)$(T.val GE 16)= -2084.681/1000;
etree_SSP1_26(T)$(T.val GE 18)= -2899.036/1000;

display etree_DICE, etree_SSP1_26, forcoth_DICE, forcoth_SSP1_26;
etree(T) = etree_SSP1_26(T);
forcoth(T) = forcoth_SSP1_26(T);
** End of changes

* For base run, this subroutine calculates Hotelling rents
* Carbon price is maximum of Hotelling rent or baseline price
* The cprice equation is different from 2013R. Not sure what went wrong.
If (ifopt eq 0,
       a2 = 0;
       solve CO2 maximizing UTILITY using nlp;
       photel(t)=cprice.l(t);
       a2 = a20;
);

cprice.up(t)$(ifopt=0 and t.val<tnopol+1) = max(photel(t),cpricebase(t));
miu.fx('1')$(ifopt=1 and ifmiulim=1) = miu0;
miu.lo('1')$(ifmiulim=0) = 0;
miu.up('1')$(ifmiulim=0) = 1;

solve co2 maximizing utility using nlp;
solve co2 maximizing utility using nlp;
solve co2 maximizing utility using nlp;

cprice.up(t) = inf;
miu.lo(t) = 0;
miu.up(t)            = limmiu;
miu.up(t)$(t.val<30) = 1;

** POST-SOLVE
** Output reported has been removed.

** Optimal Solution
ifopt = 1;
cprice.up(t)$(ifopt=0 and t.val<tnopol+1) = max(photel(t),cpricebase(t));
miu.fx('1')$(ifopt=1 and ifmiulim=1) = miu0;
miu.lo('1')$(ifmiulim=0) = 0;
miu.up('1')$(ifmiulim=0) = 1;
solve co2 maximizing utility using nlp;
solve co2 maximizing utility using nlp;
solve co2 maximizing utility using nlp;
cprice.up(t) = inf;

** 2°C target
TATM.up(T) = 2;
TATM.FX(tfirst)   = tatm0;
solve co2 maximizing utility using nlp;
solve co2 maximizing utility using nlp;
solve co2 maximizing utility using nlp;
TATM.up(T) = 12;
TATM.FX(tfirst)   = tatm0;
```

```
** 2°C Target without any climate damage
ifopt = 1;
TATM.up(T) = 2;
TATM.FX(tfirst)   = tatm0;
a2 = 0;
solve co2 maximizing utility using nlp;
solve co2 maximizing utility using nlp;
solve co2 maximizing utility using nlp;
a2 = a20;
TATM.up(T) = 12;
TATM.FX(tfirst)   = tatm0;
```

E Warming as a function of cumulative CO_2 emissions

Here we compare the multi-model mean response of the CMIP5 climate science models to the economic models, scrutinising the relationship between warming and cumulative CO_2 emissions. All the models are fed with emissions from the IPCC RCP scenarios, including both CO_2 and other greenhouse gases and forcing agents. The CMIP5 multi-model mean response is obtained from Stocker et al. (2013). The CMIP5 response is quasi-linear. By contrast, most of the economic models produce a convex response, with warming increasing more than proportionately as a function of cumulative CO_2 emissions, except for the high emissions RCP8.5 scenario and except for the Golosov et al. (2014) model. FAIR is a reasonably close approximation of the complex CMIP5 models.

Figure 8: Warming in response to cumulative CO_2 emissions, comparing the CMIP5 multi-model mean with DICE 2016

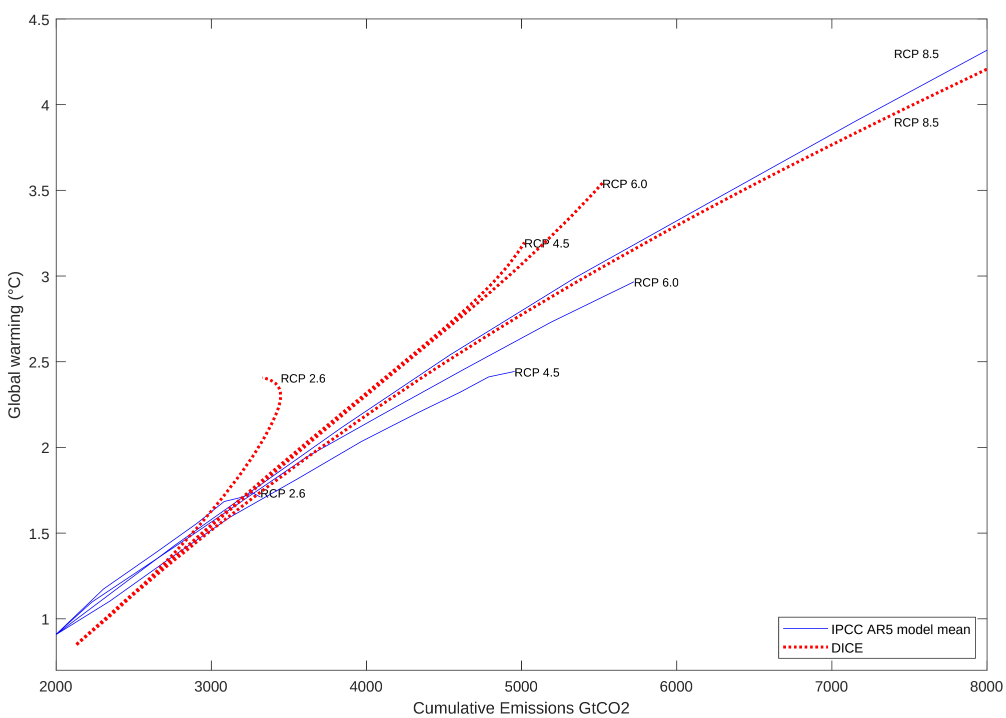

Figure 9: Warming in response to cumulative CO_2 emissions, comparing the CMIP5 multi-model mean with FUND

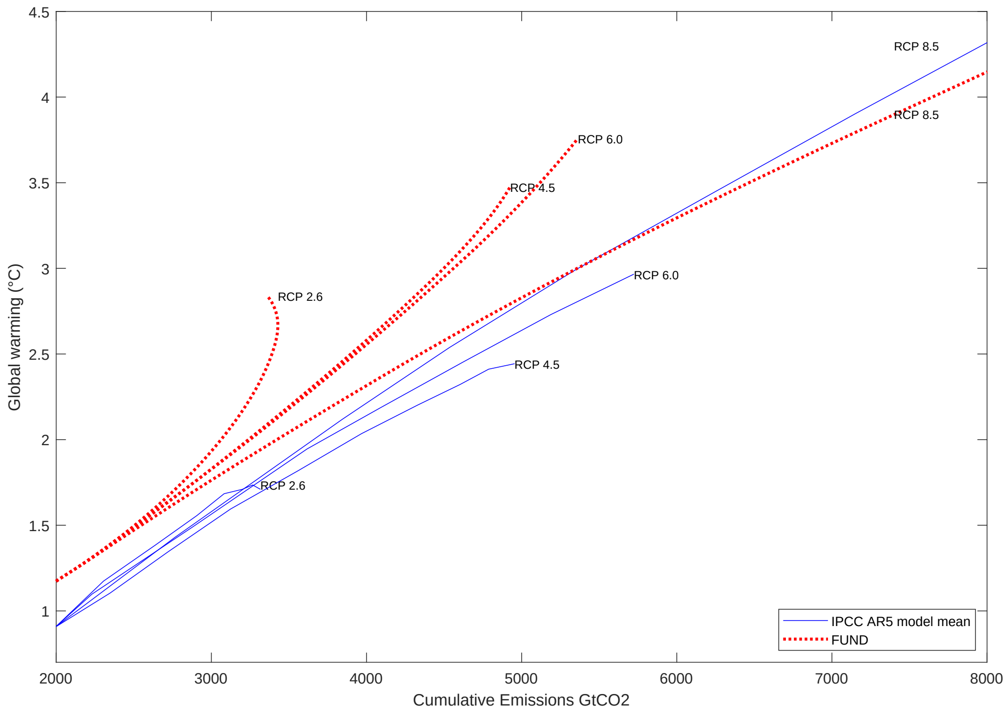

Figure 10: Warming in response to cumulative CO_2 emissions, comparing the CMIP5 multi-model mean with PAGE

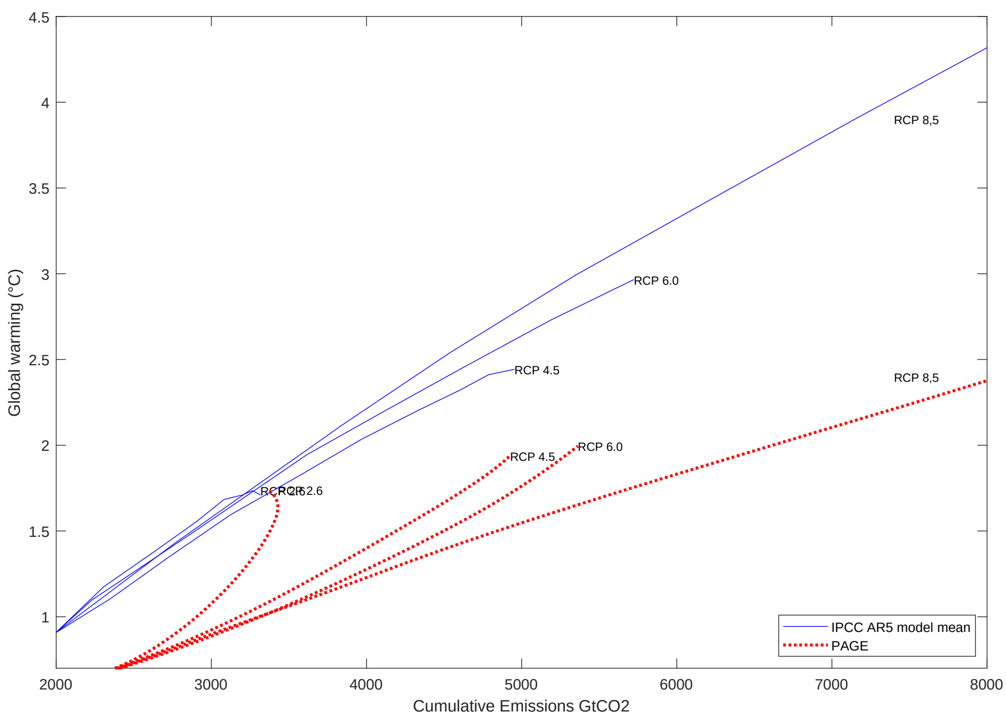

Figure 11: Warming in response to cumulative CO_2 emissions, comparing the CMIP5 multi-model mean with Golosov et al. (2014)

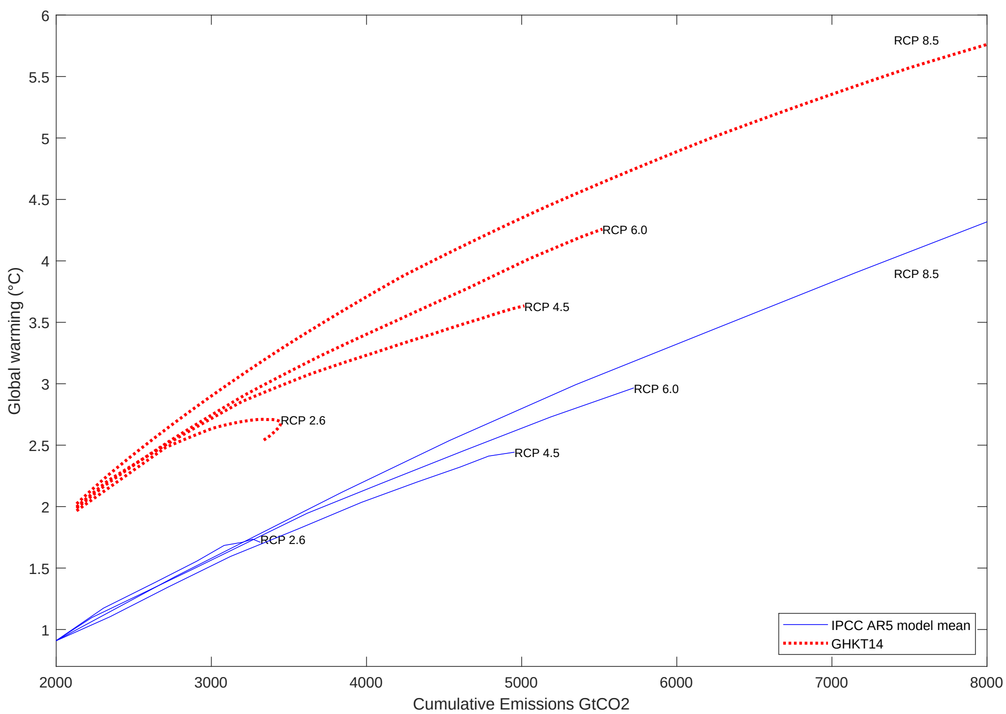

Figure 12: Warming in response to cumulative CO_2 emissions, comparing the CMIP5 multi-model mean with Gerlagh and Liski (2018)

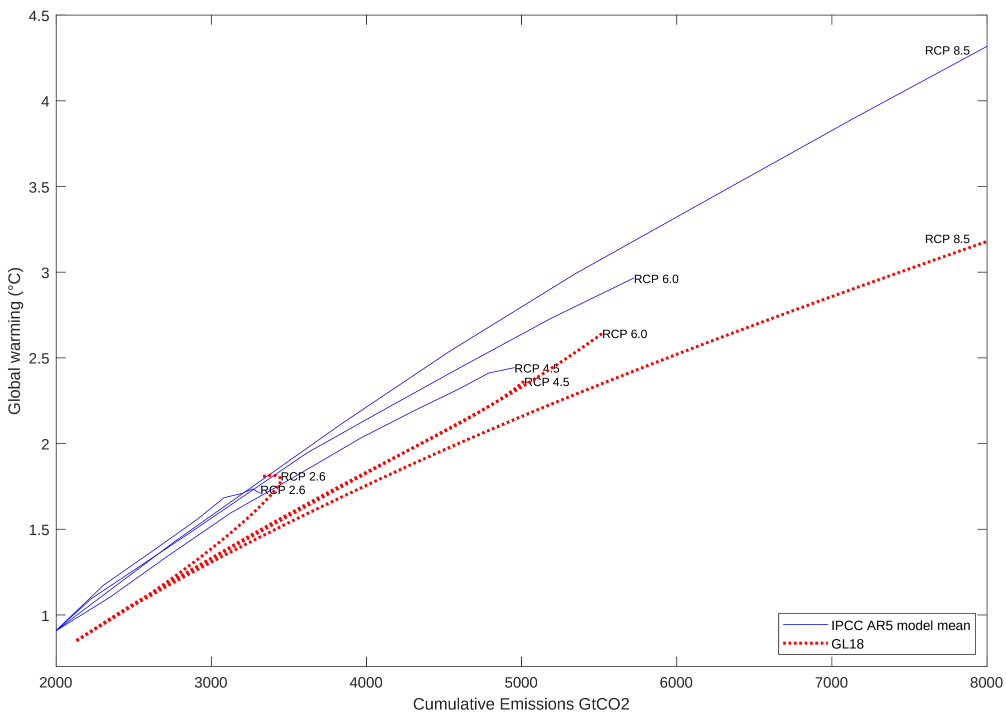

Figure 13: Warming in response to cumulative CO_2 emissions, comparing the CMIP5 multi-model mean with Lemoine and Rudik (2017)

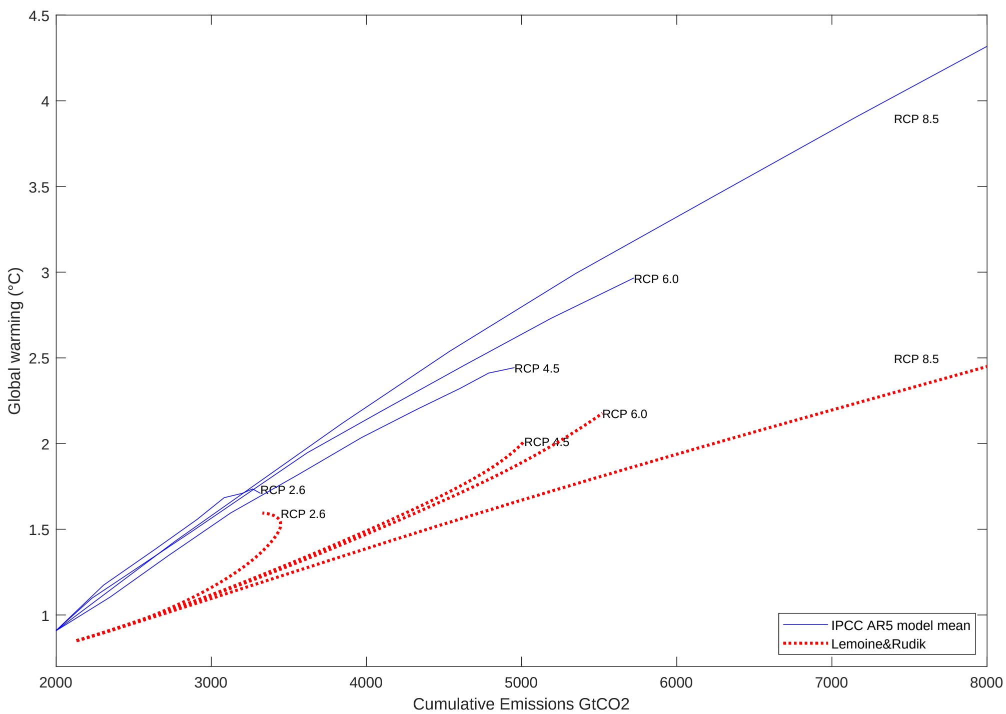

Figure 14: Warming in response to cumulative CO_2 emissions, comparing the CMIP5 multi-model mean with FAIR